Available online at www.sciencedirect.com
ScienceDirect
Journal of Organometallic Chemistry 692 (2007) 4809–4827
Journal of Organometallic Chemistry
www.elsevier.com/locate/jorganchem

Synthesis, structural characterization, and initial electroluminescent properties of bis-cycloiridiated complexes of 2-(3,5-bis(trifluoromethyl)phenyl)-4-methylpyridine

Alex S. Ionkin *,[1], Ying Wang, William J. Marshall, Viacheslav A. Petrov

DuPont Central Research & Development, Experimental Station, Wilmington, DE 19880-0328, USA

Received 21 May 2007; received in revised form 12 June 2007; accepted 12 June 2007
Available online 24 June 2007

Abstract

A series of bis-cyclometalated Ir(III) complexes (**8**–**10**, **12**, **15**, **17**, **19**, **21**, **23**, **25**, **28**, **29** and **33**) bearing two chromophoric N^C cyclometalated ligands derived from 2-(3,5-bis(trifluoromethyl)phenyl)-4-methylpyridine (**1**) and a third nonchromophoric ligand has been synthesized. A palladium-catalyzed cross-coupling reaction between 2-chloro-4-methylpyridine (**2**) and 3,5-bis(trifluoromethyl)phenylboronic acid (**3**) was used to prepare 2-(3,5-bis(trifluoromethyl)phenyl)-4-methylpyridine (**1**). Cyclometalation of (**1**) by $IrCl_3$ was carried out in $(MeO)_3P{=}O$, with the formation of chloro-bridged dimer $[N^C]_2Ir(\mu\text{-}Cl)_2Ir[C^N]_2$ (**8**). Reaction of (**8**) with lithium 2,4-pentanedionate, lithium 2,2,6,6-tetramethyl-heptane-3,5-dionate (**13**), dipivaloyltrimethylsilylphosphine (**14**), 2,2-dimethyl-6,6,7,7,8,8,8-heptafluoro-3,5-octadione (**16**), 1,1,1,3,3,3-hexafluoro-2-pyridin-2-yl-propan-2-ol (**18**), 1,1,1,3,3,3-hexafluoro-2-pyrazol-1-ylmethyl-propan-2-ol (**20**), 2-diphenylphosphanylethanol (**22**), and 1-diphenylphosphanylpropan-2-ol (**24**), afforded octahedral iridium complexes **9**, **12**, **15**, **17**, **19**, **21**, **23** and **25**, respectively. Complex **10**, which contains three different ligands ($L_1 = N^C$ of **1**; $L_2 = N^C$ of 4,4′-dimethyl-[2,2′]bipyridinyl **4**; $L_3 = O^O$ of 2,4-pentanedione), and complex **11**, which contains no cyclometalated ligands ($L_1 = \mathbf{4}$; $L_2 = L_3 = Cl$; $L_4 = O^O$ of 2,4-pentanedione) were also isolated as minor products in a one-pot reaction between a 94:5 mixture of **1** and **4**, $IrCl_3$ and lithium 2,4-pentanedionate. Reaction of **8** with diphenylphosphanylmethanol (**27**) in 1,2-dichloroethane unexpectedly led to complexes **28** and **29**. The reactions of **8** with benzoylformic acid resulted in the formation of hydroxyl-bridged dimer $[N^C]_2Ir(\mu\text{-}OH)_2Ir[C^N]_2$ (**33**). According to X-ray analyses, Ir-to-Ir distances in the crystal cell increase from 6.86 Å for **10** to 13.31 Å for **33**. The angle theta, which represents the twisting of two cyclometalated C–Ir–N planes relative to each other, varies from 97.5° for **21** to 90.76 for complex **28**. OLED devices were fabricated from several Ir complexes and preliminary results are discussed.

Keywords: Iridium; Palladium; Boron; Phosphorus; OLED; X-ray analysis

1. Introduction

Smithson Tennant discovered the element iridium over 200 years ago in the black residues remaining from the treatment of platinum ores [1]. Since then iridium has been linked to phenomena ranging from the disappearance of dinosaurs [2] to organic light emitting diodes [3]. In particular, mono-cyclometalated (N^C) Pt^{II} complexes (Type **a** in the Scheme 1) and bis-cyclometalated (N^C) complexes of Ir^{III} with 2-phenylpyridine ligands (Type **b** in the Scheme 1) have been widely investigated as promising electroluminescent materials for OLED applications.

Emission colors from these Pt and Ir complexes range from blue-green, to green and to red, and depend mostly on the choice of the chromophoric cyclometalated ligand. The electronic parameters and steric bulk of the second, nonchromophoric ligands are also important for the color coordinate and intensity of the emission. For example,

* Corresponding author. Tel.: +302 6952968; fax: +302 6958281.
E-mail address: alex.s.ionkin@usa.dupont.com (A.S. Ionkin).
[1] This is DuPont contribution #8711.

0022-328X/$ - see front matter © 2007 Elsevier B.V. All rights reserved.
doi:10.1016/j.jorganchem.2007.06.026

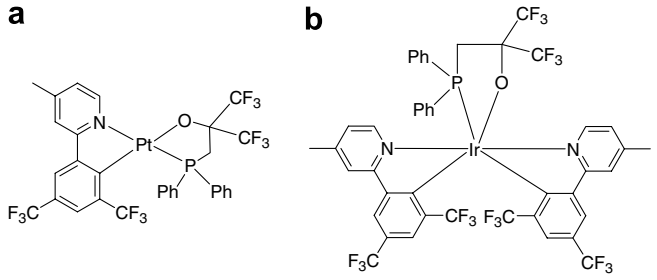

Scheme 1.

increasing the steric bulk of the secondary auxiliary ligands in Pt-complexes (Type **a** in Scheme 1) shifted the emission wavelength to higher energies (from 600 nm to 540 nm) [4]. Introduction of P^O ligands was found to shift the emission to the blue part of the spectrum [5]. Blue emissive materials are among the most sought after components for the emerging OLED market.

In this report, we studied the effect of varying the third ligand in bis-cyclometalated Ir-complexes (Type **b** in Scheme 1). An attempt was made to correlate structural features of the bis-cyclometalated moiety of the iridium complexes with the final electroluminescent spectra. Such bis-cyclometalated iridium complexes are highly crystalline substances, which greatly facilitated X-ray analysis. Frequently, electrochemical and photochemical studies, as well as theoretical calculations, have been used to interpret the blue shift in OLED devices [3–5]. 2-(3,5-Bis(trifluoromethyl)-phenyl)-4-methylpyridine **1** was selected as a ligand for cycloiridation because it is easily prepared and it provides intensive blue emissive bis-cyclometalated Ir(III) complexes [5].

2. Results and discussion

2.1. Synthesis of bis-cyclometalated Ir(III) complexes and structural studies

*2.1.1. Synthesis of 2-(3,5-bis(trifluoromethyl)phenyl)-4-methylpyridine **1***

The palladium-catalyzed Suzuki cross-coupling reaction between 2-chloro-4-methylpyridine (**2**) and 3,5-bis(trifluoromethyl)phenylboronic acid (**3**) was used to prepare 2-(3,5-bis(trifluoromethyl)phenyl)-4-methylpyridine (**1**) (Schemes 2, 3). Two catalytic protocols were tested. The first one (Scheme 2) involves the tetrakis(triphenylphosphine)palladium(0) as the catalyst in the presence of potassium carbonate and a mixture of monoglyme (1,2-dimethoxyethane)/water as solvent. This protocol is attractive for its simplicity and the commercial availability of all reagents [6].

2-(3,5-Bis(trifluoromethyl)phenyl)-4-methylpyridine (**1**) was isolated by the distillation, together with some (<5%) 4,4′-dimethyl-[2,2′]bipyridinyl (**4**). One explanation for the formation of compound **4** can be found in the general Suzuki catalytic cycle [6]. The intermediate formed by the

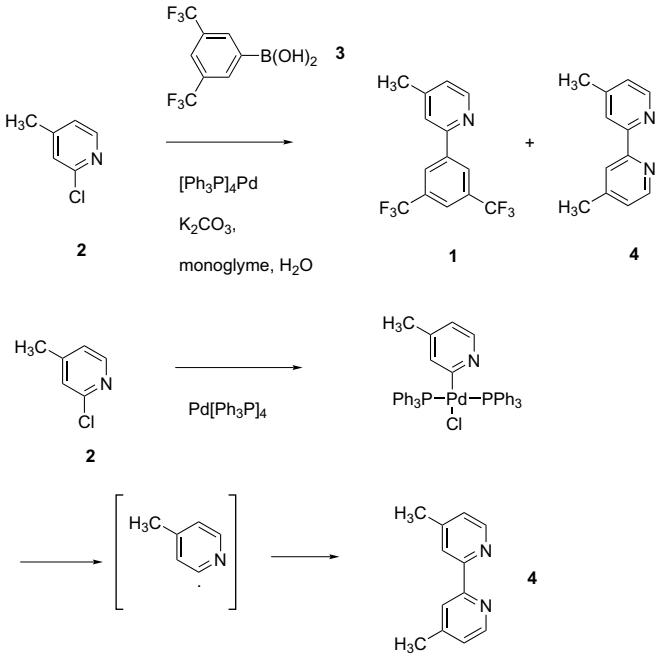

Scheme 2.

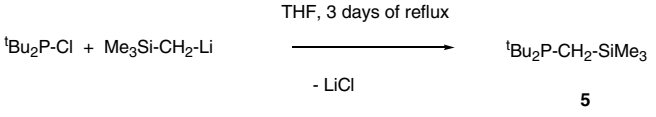

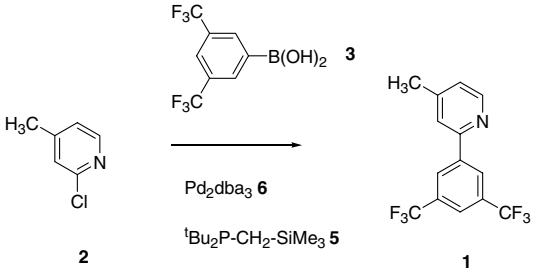

Scheme 3.

oxidative addition of 2-chloro-4-methylpyridine to tetrakis(triphenylphosphine)palladium(0) may undergo elimination of a 4-methylpyridinyl-2 radical with sequential dimerization to afford the 4,4′-dimethyl-[2,2′]bipyridinyl (second reaction in Scheme 2). A second possibility is that 2-chloro-4-methylpyridine reacted with the first intermediate in the Suzuki reaction to yield 4,4′-dimethyl-[2,2′]bipyridinyl.

Bipyridinyl **4** is able to participate in cyclometalation reactions, as was noted by Lepeltier and coauthors [7]. Consequently, an alternative synthesis of **1** was developed utilizing di-*tert*-butyl-trimethylsilylanylmethylphosphine (**5**) and Pd_2dba_3 **6** as the catalyst (Scheme 3). This catalytic protocol has proved to be quite reliable [8]. The di-*tert*-

butyl-trimethylsilylanylmethylphosphine (**5**), used in this process, was synthesized by prolonged reflux of equimolar amounts of di-*tert*-butylchlorophosphine and (trimethylsilylmethyl)lithium in THF, and then purified by distillation under vacuum.

The above synthetic protocol uses cesium fluoride **7** as a base and 1,4-dioxane as the solvent [8]. Yield of 2-(3,5-bis(trifluoromethyl)phenyl)-4-methylpyridine (**1**) by this second method was 91.0% after purification by chromatography on silica gel. No evidence of contamination by bipyridinyl **4** was observed.

2.1.2. Synthesis of bis-cyclometalated derivatives (*8–10, 12, 15, 17, 19, 21, 23, 25, 28, 29 and 33*)

Bis-cyclometalation of 2-(3,5-bis(trifluoromethyl)-phenyl)-4-methylpyridine (**1**) was carried out in trimethylphosphate [9]. The Ir^{III}-bridged di-chloride dimer **8** usually precipitated from the trimethylphosphate solution, which simplified the purification step (Scheme 4).

One-pot bis-cyclometalation of 2-(3,5-bis(trifluoromethyl)phenyl)-4-methylpyridine **1** (prepared by the first catalytic protocol and containing 4,4′-dimethyl-[2,2′]bipyridinyl), followed by reaction with lithium 2,4-pentanedio-

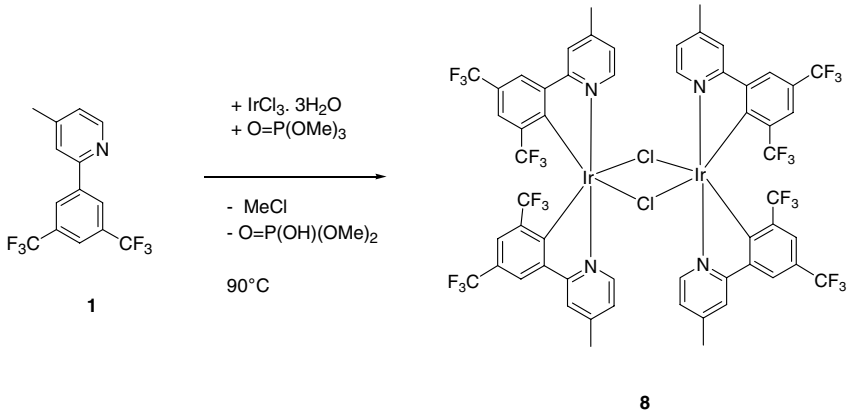

Scheme 4.

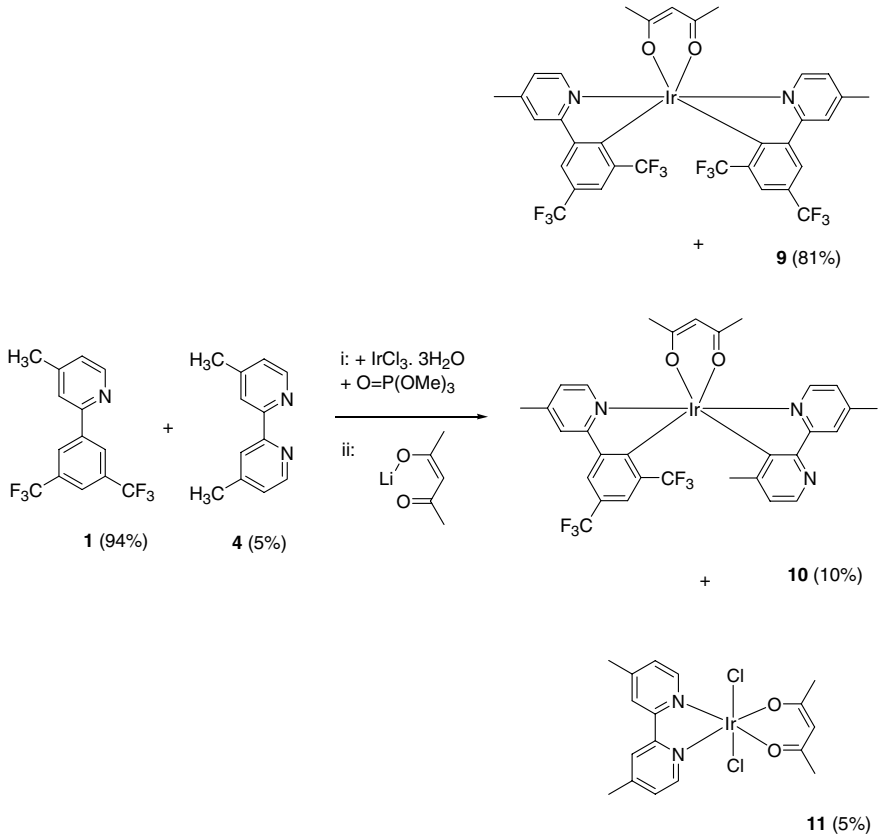

Scheme 5. One-pot syntheses of Ir-complexes **9**–**11**.

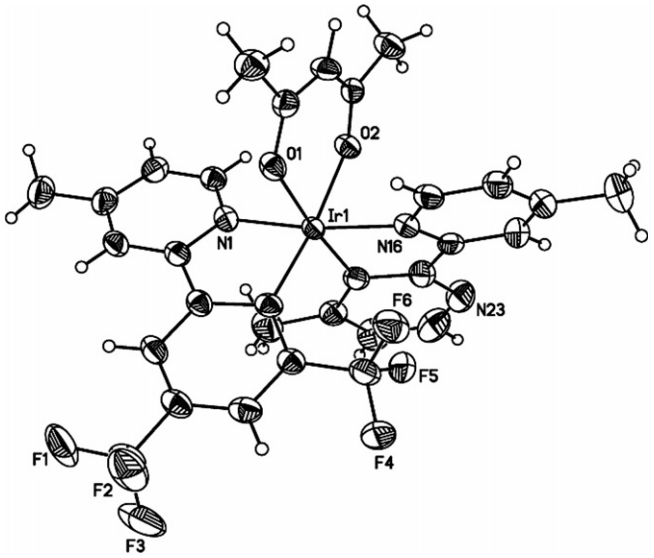

Fig. 1. ORTEP drawing of iridium,bis[4,6-bis(trifluoromethyl)-2-(4-methyl-2-pyridinyl-κN)phenyl-κC](2,4-pentanedionato-κ*O*,κ*O*′) (**10**). Thermal ellipsoids are drawn to the 50% probability level.

nate, resulted in the isolation of three complexes (**9**–**11**, Scheme 5).

The target bis-cyclometalated complex **9** was the major product, and was separated by chromatography on silica gel in 81% yield. Complex **10**, which contains three different ligands, was isolated with 10% yield. An ORTEP drawing of compound **10** as the *trans-N,N*-isomer is shown in Fig. 1.

Complex **11**, which contains no cyclometalated ligands, was a minor product of the one-pot reaction. Its structure was investigated by X-ray analysis (Fig. 2). The formation of **11** can be explained by the initial coordination of one equivalent of bipyridinyl **4** with iridium(III) chloride, and the sequential Cl/O^O ligand exchange reaction of the

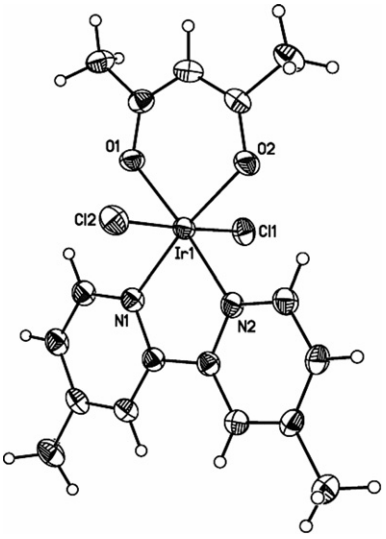

Fig. 2. ORTEP drawing of iridium,dichloro[4,4′-dimethyl-[2,2′]bipyridinyl-κN1,κN1],(2,4-pentanedionato-κ*O*,κ*O*′) (**11**). Thermal ellipsoids are drawn to the 50% probability level.

formed intermediate with one equivalent of lithium 2,4-pentanedionate.

The rest of the cyclometalated complexes were prepared from the 2-(3,5-bis(trifluoromethyl)phenyl)-4-methylpyridine (**1**) synthesized by the second catalytic protocol (Scheme 3). Syntheses of the additional bis-cyclometalated complexes from the subclass of O^O auxiliary ligands are shown in Scheme 6. Thus, iridium, bis[4,6-bis(trifluoromethyl)-2-(4-methyl-2-pyridinyl-κN)phenyl-κC](2,2,6,6-tetramethyl-3,5-heptanedionato-κ*O*,κ*O*′)-(**12**) was synthesized by the reaction of complex **8** and lithium 2,2,6,6-tetramethyl-heptane-3,5-dionate (**13**). Complex **12** is analogous to complex **9**, but was designed to have bulkier *tert*-butyl groups instead of methyl groups to provide greater separation of the complexes from each other in the solid state. A crystal of complex **12** suitable for X-ray analysis was grown from pentane. An ORTEP drawing of **12** is shown in Fig. 3. 2,2,6,6-Tetramethyl-heptane-3,5-dionate was replaced as the third ligand with dipivaloyltrimethylsilylphosphine (**14**), to test the impact of incorporating a phosphorus lone pair in the center of acetylacetonate ligand. Compound **14** was prepared by the condensation of tris(trimethylsilyl)phosphine with pivaloyl chloride [10]. Refluxing complex **8** with dipivaloyltrimethylsilylphosphine **14** gave complex **15** after purification by chromatography on silica gel. According to the X-ray analysis, **15** contains the two-coordinated phosphorus atom in an analogue of an acetylacetonate ligand (Fig. 4). The ^{31}P NMR spectrum of **15** contains a downfield chemical shift at 50.97 ppm, which is similar to two-coordinated phosphorus atoms incorporated in 2-phospha-1,3-dionate fragments of Ni and B-complexes [11]. To explore the effect of electron-withdrawing groups in the third O^O auxiliary ligand, fluorinated derivatives were prepared. Reaction of 2,2-dimethyl-6,6,7,7,8,8,8-heptafluoro-3,5-octadione **16** with complex **8** produced iridium, bis[4,6-bis(trifluoromethyl)-2-(4-methyl-2-pyridinyl-κN)phenyl-κC],(6,6,7,7,8,8,8-heptafluoro-2,2-di-methyl-3,5-octanedionato-κ*O*,κ*O*′)- (**17**).

Syntheses of the bis-cyclometalated complexes belonging to the subclass with N^O auxiliary ligands are shown in Scheme 7. Thus, use of 1,1,1,3,3,3-hexafluoro-2-pyridin-2-yl-propan-2-ol (**18**) led to the isolation of complex **19** with a five-membered N^O ring. The reaction between 1,1,1,3,3,3-hexafluoro-2-pyrazol-1-ylmethyl-propan-2-ol (**20**) and complex **8** gave the corresponding pyrazol complex **21** with a six-membered N^O ring. An ORTEP drawing of **21** can be seen in Fig. 5. The compound exists as the *trans-N,N*-isomer, which seems to be the predominant configuration for this particular cyclometalated phenylpyridine.

Syntheses of the bis-cyclometalated complexes belonging to the subclass with P^O auxiliary ligands are shown in Scheme 8. In order to determine if the fluorinated phosphine in complex type **b** (Scheme 1) is the only P^O ligand to form blue emissive iridium complexes, a few inexpensive β-oxyalkyldiphenylphosphines were tested. The simplest representative of β-oxyalkyldiphenylphosphines

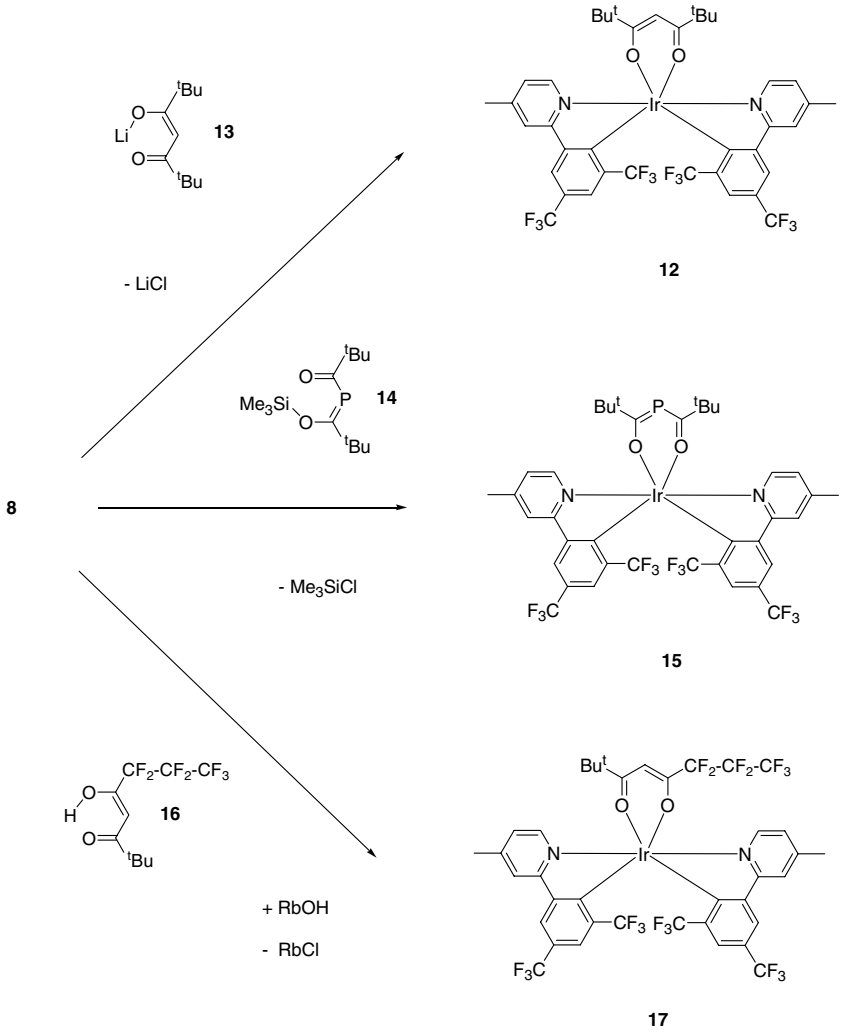

Scheme 6. Syntheses of O^O derivatives of **12**, **15** and **17**.

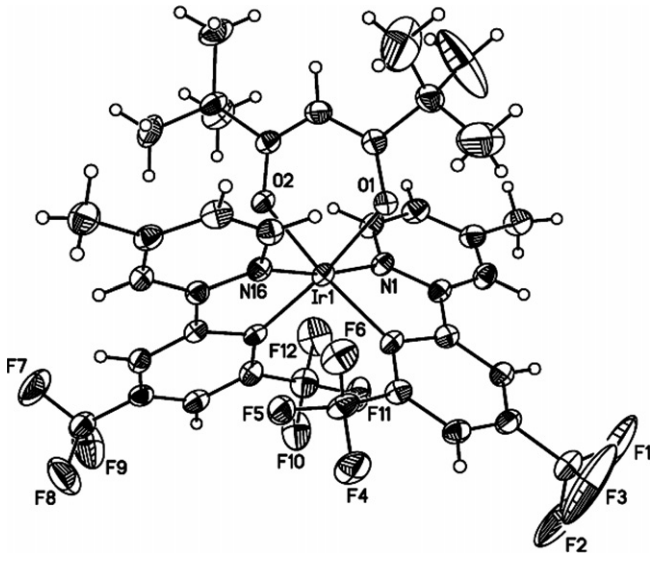

Fig. 3. ORTEP drawing of iridium, bis[4,6-bis(trifluoromethyl)-2-(4-methyl-2-pyridinyl-κN)phenyl-κC](2,2,6,6-tetramethyl-3,5-heptanedionato-κ*O*, κ*O′*) (**12**). Thermal ellipsoids are drawn to the 50% probability level.

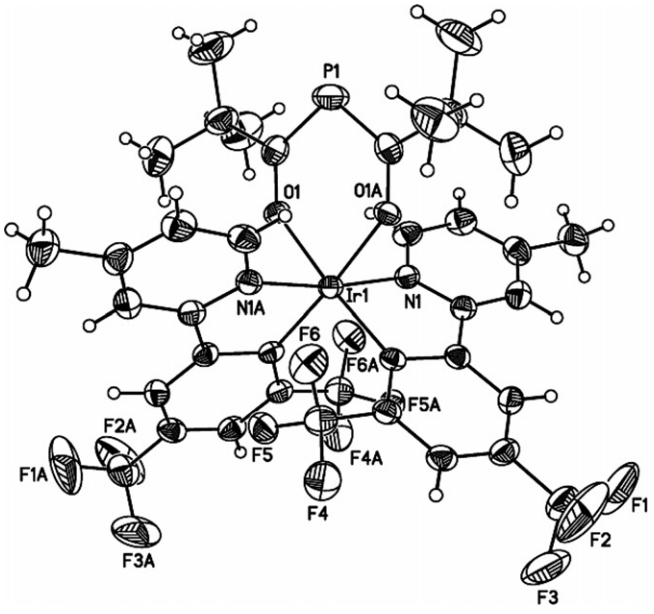

Fig. 4. ORTEP drawing of iridium, bis[4,6-bis(trifluoromethyl)-2-(4-methyl-2-pyridinyl-κN)phenyl-κC],((2,2-dimethyl-1-oxopropyl)phosphinato-*O*,*O′*) (**15**). Thermal ellipsoids are drawn to the 50% probability level.

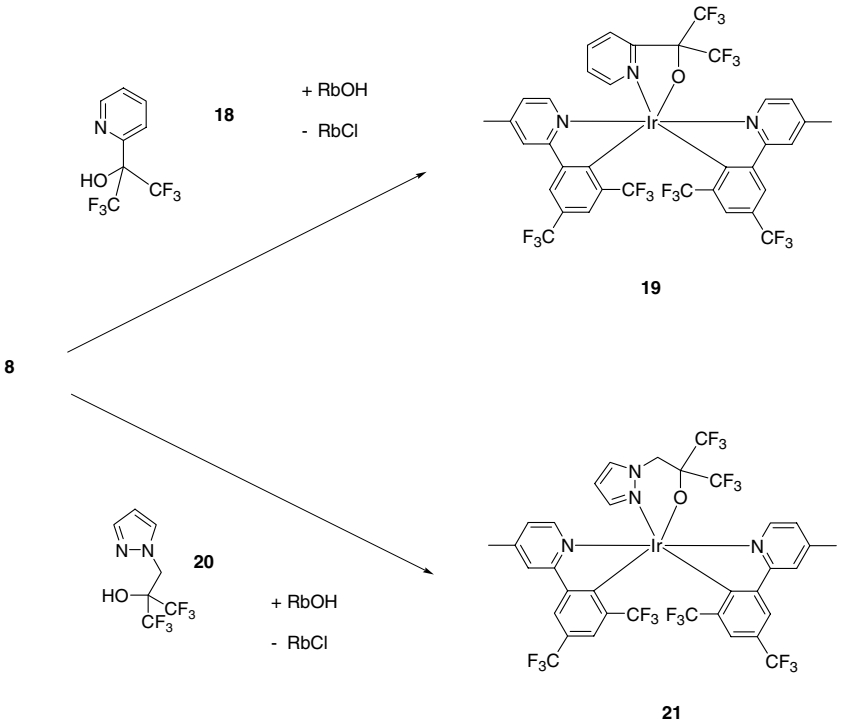

Scheme 7. Syntheses of N^O derivatives of **19** and **21**.

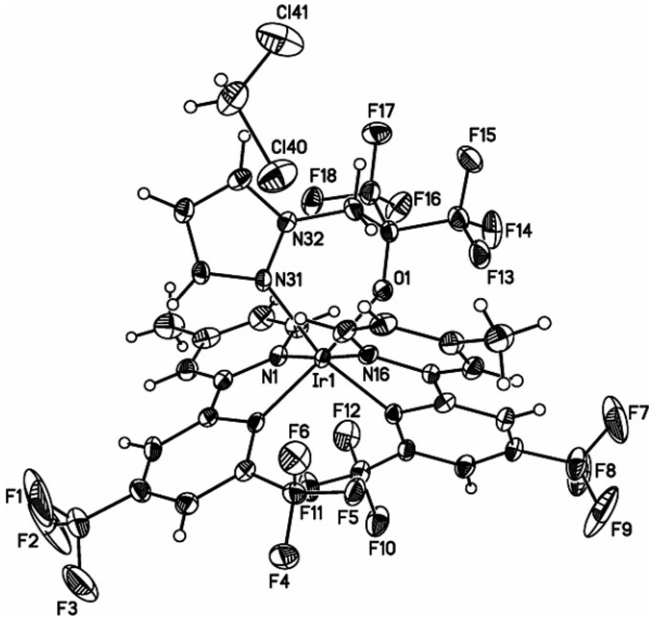

Fig. 5. ORTEP drawing of iridium,bis[4,6-bis(trifluoromethyl)-2-(4-methyl-2-pyridinyl-κN)phenyl-κC],[α,α-bis(trifluoromethyl)-2-pyrazol-1-ylmethyl-propan-2-olato-κN1,κO2] (**21**). Thermal ellipsoids are drawn to the 50% probability level.

is 2-diphenylphosphanyl-ethanol (**22**). It gave complex **23** upon reaction with parent complex **8**. A crystal suitable for X-ray analysis was grown from methanol, which forms two hydrogen bonds with the oxygen of phospholane cycle of **23**. An ORTEP of **23** is shown in Fig. 6. 1-Diphenylphosphanylpropan-2-ol (**24**) underwent a cyclization reaction upon the reaction with **8** to give complex **25**. An ORTEP drawing of **25** (Fig. 7) shows the P^O coordination mode and the formation of a five-membered ring.

To assess the impact of the size of the P^O chelating ligand on the emission color, the synthesis of a bis-cyclometalated complex with a four-membered ring instead of a five-membered ring was attempted (compare complex **26** and **23** in following Scheme 9). Diphenylphosphanylmethanol (**27**) was used in a Cl/P^O ligand exchange reaction. Instead of compound **26**, photo-emissive complexes **28** and **29** were isolated (Scheme 10 and Figs. 8 and 9). Complex **28** formed from complexation with diphenylphosphine (**30**), which can be derived from the retro reaction of diphenylphosphanylmethanol (**27**), in which formaldehyde is eliminated (Scheme 11) [12].

The formation of 1,2-ethanediylbis(diphenylphosphine) complex **29** is not as easy to explain. Presumably, the driving force for the formation **29** is stabilization of a cationic iridium complex by the two phosphorus atoms in 1,2-bis(diphenylphosphino)ethane (**31**). One possibility is that in the presence of a strong base (RbOH), diphenylphosphine (**30**) reacted with the solvent (dichloroethane) to form 1,2-bis(diphenylphosphino)ethane (**31**). A second possibility is that diphenylphosphanyl-methanol (**27**) reacted with dichloroethane and eliminated formaldehyde to form biphosphine (**31**). The formation of tertiary phosphines from alkyl halides in the presence strong bases (e.g., CsOH) is known [13]. It seems that four-membered ring systems incorporating Ir are less favorable than five-membered ring systems.

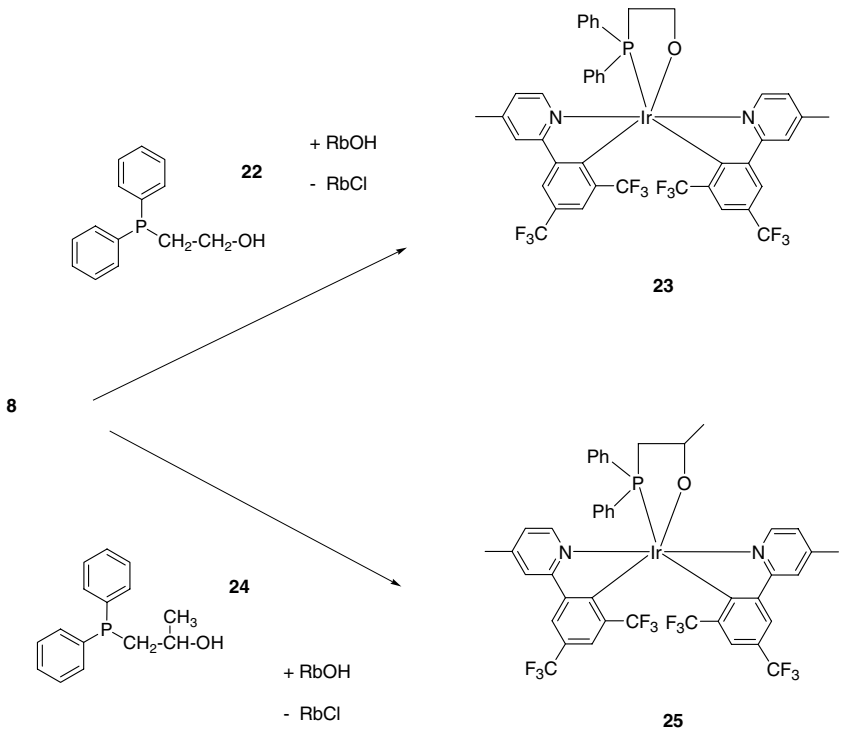

Scheme 8. Syntheses of P^O derivatives of **23** and **25**.

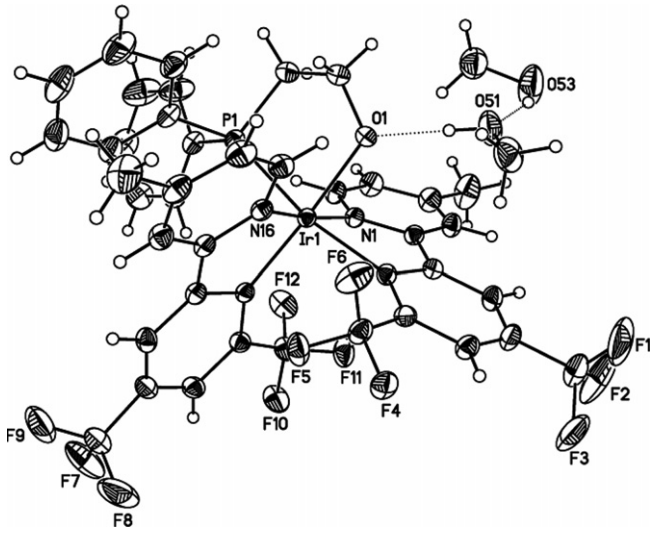

Fig. 6. ORTEP drawing of iridium,bis[4,6-bis(trifluoromethyl)-2-(4-methyl-2-pyridinyl-κN)phenyl-κC],[3-(di-phenylphosphino)-1-propanolato-*O*,*P*] (**23**). Thermal ellipsoids are drawn to the 50% probability level.

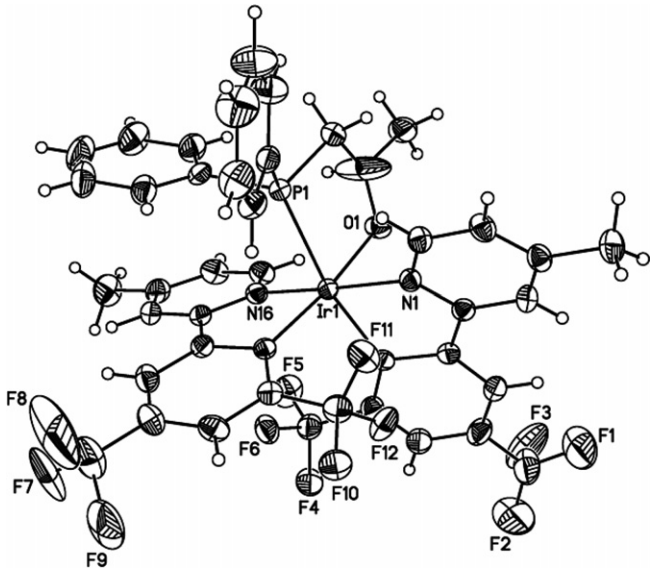

Fig. 7. ORTEP drawing of iridium,bis[4,6-bis(trifluoromethyl)-2-(4-methyl-2-pyridinyl-κN)phenyl-κC], [1-(di-phenylphosphino)-2-propanolato-*O*,*P*] (**25**). Thermal ellipsoids are drawn to the 50% probability level.

In an attempt to make other five-membered rings containing Ir, benzoylformic acid was reacted with compound **8**. Iridium, di-μ-hydroxytetrakis[4,6-bis(trifluoromethyl)-2-(4-methyl-2-pyridinyl-κN)phenyl-κC]di- (**33**) was isolated as a major product (Scheme 12 and Fig. 10). Decarbonylation and decarboxylation of the benzoylformic moiety of **32** in the presence of water likely account for the formation of **33** [14]. Benzene and benzaldehyde were identified by the ^{1}H NMR spectrometry during the monitoring of this reaction. An alternative mechanism for the formation of **33** is the replacement of Ir–Cl bonds in **8** with Ir-OH bonds by a strong base (e.g., RbOH). Although the X-ray and ^{1}H NMR analyses did not locate the hydrogen atoms at the oxygens, the IR-spectrum of complex **33** contains a broad band at 3445 cm^{-1} corresponding to IrOH groups [15].

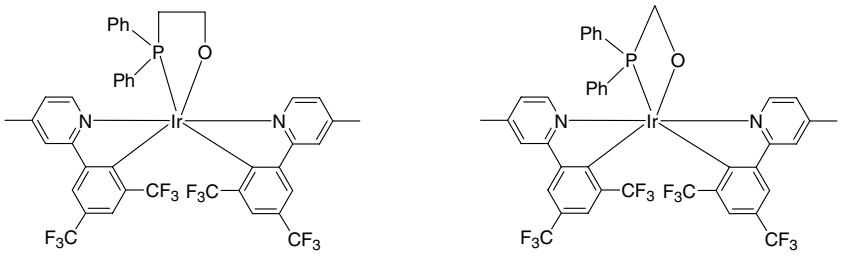

23 26

Scheme 9.

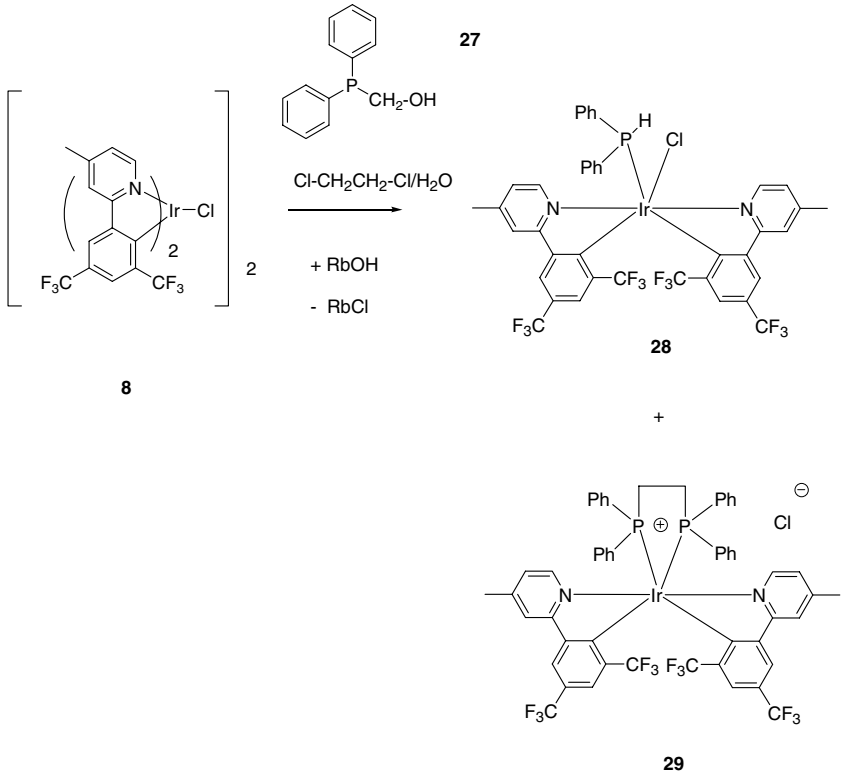

Scheme 10.

2.2. Structural studies of the bis-cyclometalated derivatives

X-ray analysis of bis-cyclometalated complexes containing ligands derived from 2-(3,5-bis(trifluoromethyl)-phenyl)-4-methylpyridine reveals that in all cases the two chromophoric cyclometalated ligands exist in an *N*,*N*-*trans* configuration (Scheme 13). The third ligand does not alter the octahedral geometry around the iridium atom. Crystallographic data are presented in Tables 1–5.

Ir–N bond lengths in the analyzed complexes vary from 2.023 to 2.067 Å, and are within the normal range for bis-cyclometalated complexes based on 2-phenylpyridine ligands [16]. The Ir–C bond lengths (from 2.012 to 2.111 Å) are also within the range found for other Ir–C bonds with the same 2-phenylpyridine ligands [17,18].

The angle theta is calculated as 180° minus the angle between the vectors normal to each of the C–Ir–N planes as calculated using the SHELXTL-XP program. This represents the twisting of the C–Ir–N planes relative to each other. Higher angular values are representative of a greater distance between the phenyl rings (Table 1).

The Pt–Pt distance in π–π stacked cyclometalated complexes is an important parameter that affects the color coordinates of OLED devices that incorporate mono-cyclometalated Pt complexes [4]. It should be pointed out that there are no π–π stacking interactions in the Ir-complexes discussed in this study. However, Ir–Ir distances of non-stacked molecules can be useful and can represent sterical bulk around the Ir core created by the three ligands.

3. Electroluminescent properties of Bis-cyclometalated Ir(III) complexes 9, 12, 19, 21, 23, and 25

Preliminary device work was done using iridium complexes **9**, **12**, **19**, **21**, **23**, and **25** as the electroluminescent emitters [3,19–34]. The device configuration consists of

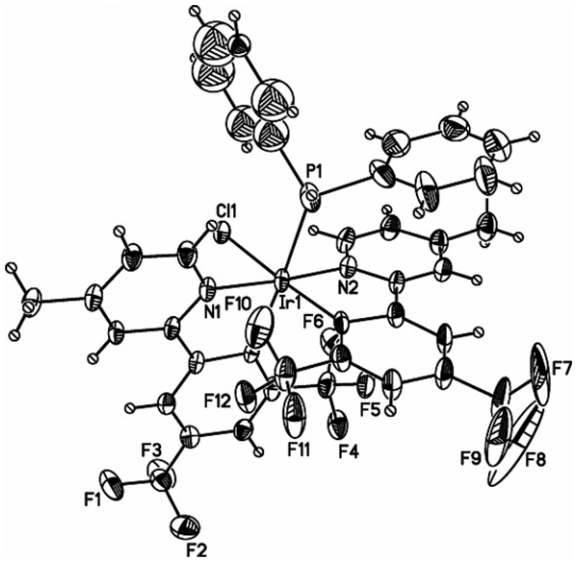

Fig. 8. ORTEP drawing of iridium,chlorobis[4,6-bis(trifluoromethyl)-2-(4-methyl-2-pyridinyl-κN)phenyl-κC],[diphenylphosphine] (**28**). Thermal ellipsoids are drawn to the 50% probability level.

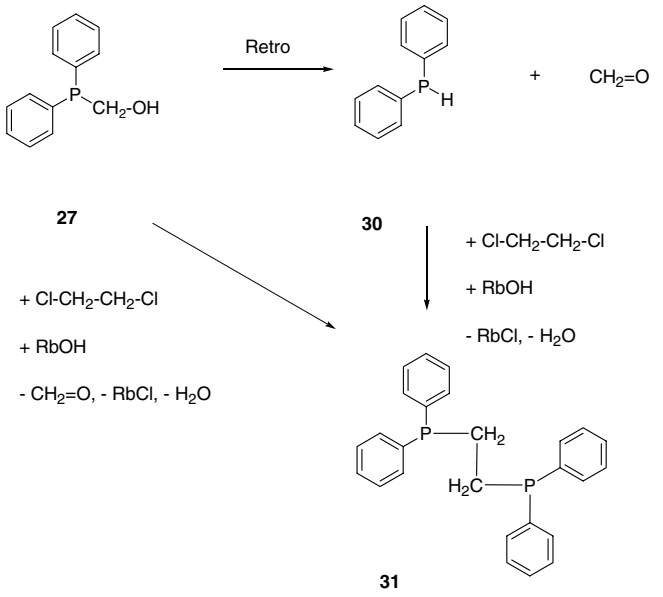

Scheme 11.

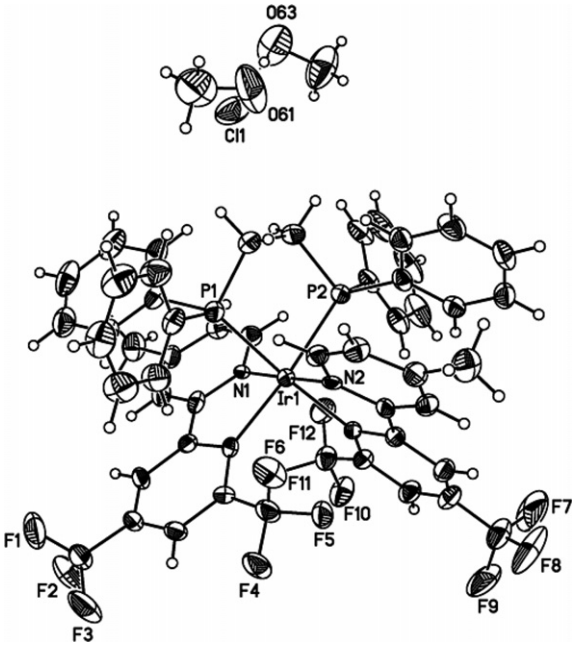

Fig. 9. ORTEP drawing of chlorobis[4,6-bis(trifluoromethyl)-2-(4-methyl-2-pyridinyl-κN)phenyl-κC],[1,2-ethanediylbis[diphenylphosphine-κP] (**29**). Thermal ellipsoids are drawn to the 50% probability level.

ITO as the anode, MPMP (50 nm) as the hole transport material, Ir emitters (40 nm), DPA (40 nm) as the electron transport material, and LiF/Al as the cathode. This device configuration has been proved to be a very efficient to scout the Ir-based emitters [8a]. Molecular structures of MPMP, AlQ and DPA are shown in the Scheme 14.

Electroluminescent spectra are displayed in Fig. 11. All compounds give bluish electroluminescence, with the shortest wavelength peak at 470 nm, followed by vibronic progression with peaks at ~505 nm and 540 nm (Fig. 11). Although the third ligands of these Ir compounds vary considerably, the electroluminescence spectra are dominated by the luminophore, the 2-(3,5-bis(trifluoromethyl)-phenyl)-4-methylpyridine ligand. The third ligand does, however, affect the shape of the electroluminescent spectra. Compounds **9**, **23**, and **25**, in particular, show broadened spectra. This spectral broadening may be caused by either interaction of the luminophore in the solid state or the Fabry–Perot interference effect [35]. The second effect is an optical effect arising from luminescence circulating in the cavity formed by the ITO and Al electrode, which can affect the spectrum due to positive and negative interference. All devices used the same layer thickness, so this Fabry–Perot effect should be substantially the same for all compounds. Nevertheless, there could be a slight difference in the n and k values for these compounds, which could cause a small difference of the Fabry–Perot effect and therefore a small modification to the spectrum. We expect the major contribution to the spectral broadening seen in Fig. 11 to have come from the interaction of the luminophore in the film. The extent of the broadening can be approximately represented by the full-width-half-maximum of the spectra, which is listed in Table 1 for various Ir compounds. Within the same subclasses of the third ligand, the spectral broadening tends to decrease with increasing steric bulk of the complexes. For example, moving from the less sterically hindered methyl-substituted acac derivative (O^O) **9** to the more sterically hindered *tert*-butyl-substituted derivative **12**, the full-width-half-maximum decreased from 80 to 55 nm. The first closest Ir–Ir distances (Table 1) may be used to approximate the relative bulk of these complexes. The Ir–Ir distance also appears to correlate with the full-width-half-maximum of the spectrum within the same subclass of complexes. For example, compound **12** has the narrowest luminescence

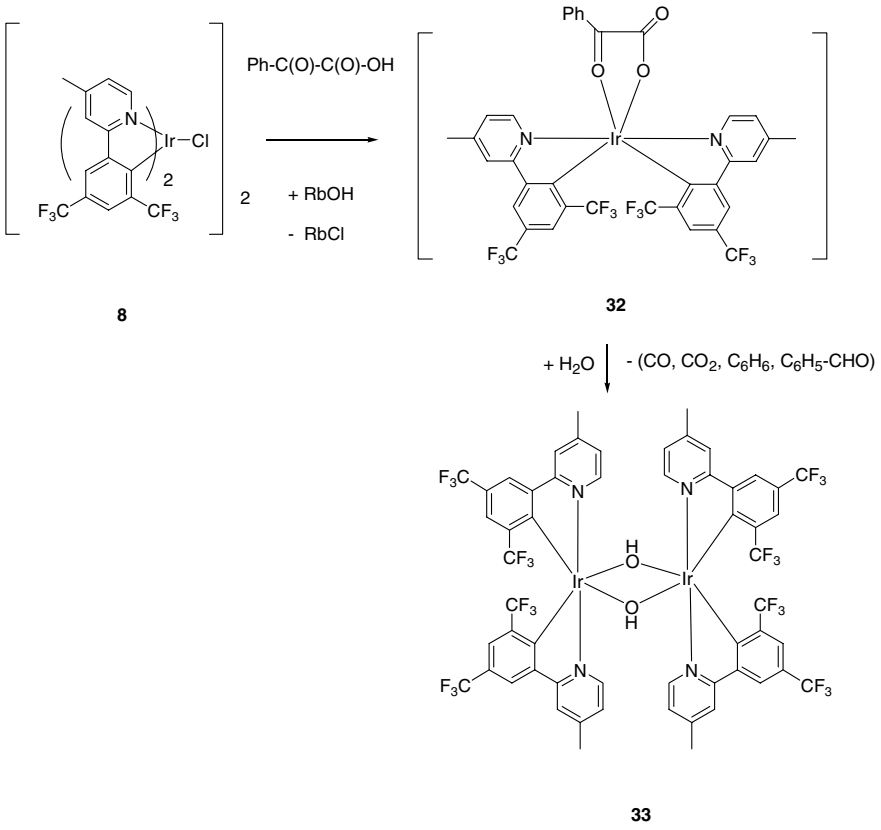

Scheme 12.

band and the longest Ir–Ir distance (9.66 Å); compounds **9**, **19**, and **25** have broader luminescence bands and shorter Ir–Ir distances (8.41–8.86 Å).

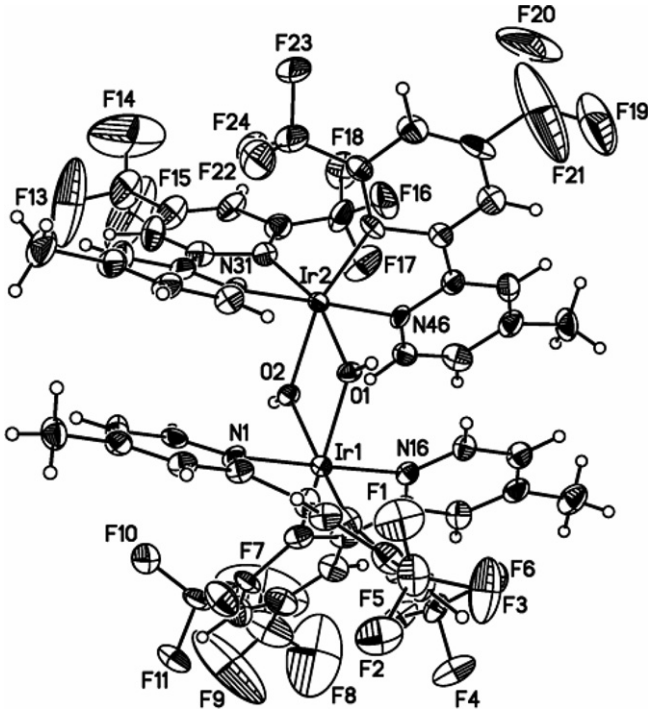

Fig. 10. ORTEP drawing of iridium, di-μ-hydroxytetrakis[4,6-bis(trifluoromethyl)-2-(4-methyl-2-pyridinyl-κN)phenyl-κC]di (**33**). Thermal ellipsoids are drawn to the 50% probability level.

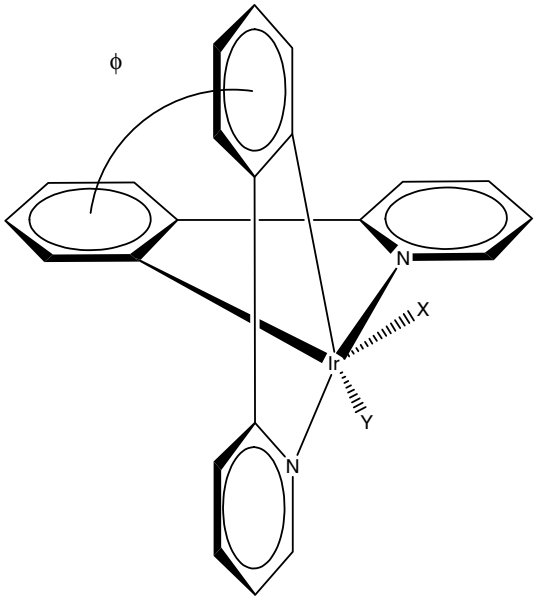

Scheme 13. Notable features of the bis-cyclometalated complexes **9**, **12**, **19**, **21**, **23**, **25** and **28**. The nonchromophoric ligands are marked as "X" and "Y" for the best visual representation of angle theta. The angle theta represents the orientation of two cyclometalated C^N ligands relative to each other. All complexes are *trans-N,N*-isomers and octahedral.

Electroluminescent device data for these compounds are summarized in Table 1. Compound **21** gives a high electroluminescent efficiency of 8 cd/A without any device optimi-

Table 1
Summary of electroluminescent properties of complexes **9**, **12**, **19**, **21**, **23**, **25** and angle theta, and the first closest Ir–Ir distances (Å) in the crystal cell

Complex	Efficiency (cd/A)	Peak radiance (cd/m^2)	Full-width-half-maximum of electroluminescence spectra (nm)	The first closest Ir–Ir distance (Å)	Angle theta
21	8.5 at 18 V	1800	60	9.44	97.5
19	2 at 15 V	800	70	8.41	95.2
12	2.5 at 19 V	420	55	9.66	94.56
25	2.5 at 17 V	400	75	8.68	94.76
9	3.5 at 21 V	350	80	8.86	94.6
23	0.6 at 21 V	60	80	9.39	92.58

zation. The efficiency vs. voltage and current vs. voltage curves are plotted in Fig. 12. There is an interesting qualitative correlation between the device efficiency/radiance and the shape of the spectra. The worst performing emitter, compound **23**, has a rather broad and smeared out spectrum, indicating significant interaction in the film. The best performing emitter, compound **21**, shows well-defined vibronic peaks, indicating weaker intermolecular interaction. Furthermore, there is an apparent correlation between the radiance and the theta angle. Compound **23** has the smallest theta angle and the lowest efficiency and radiance, while compound **21** has the largest theta angle and the highest efficiency and radiance. The exact reason behind this apparent correlation is not clear, but may be connected with the luminescence yield of these compounds.

4. Summary and conclusions

A series of bis-cyclometalated Ir(III) complexes bearing two chromophoric N^C cyclometalated ligands (2-(3,5-bis(trifluoromethyl)phenyl)-4-methylpyridine (**1**)) and a variety of nonchromophoric O^O, N^O, P^O, P^Cl, P^P compounds as the third ligands was synthesized. The peak wavelengths of OLED devices prepared from these Ir complexes (470 nm) are determined by the cyclometalated ligand. Variation of the third ligand does not change the peak position, but has some effect on the spectral shape due to changes in intermolecular packing. Within the same subclasses of the third ligand, the spectral broadening tends to decrease with increasing steric bulk of the complexes.

Table 2
Summary of crystal data, data collection, and structural refinement parameters for **9**, **10**, **11** and **12**

	9	**10**	**11**	**12**
Empirical formula	$C_{33}H_{23}F_{12}IrN_2O_2$	$C_{64}H_{56}Cl_4F_{12}Ir_2N_6O_4$	$C_{17}H_{19}Cl_2IrN_2O_2$	$C_{39}H_{35}F_{12}IrN_2O_2$
FW	899.73	1727.35	546.44	983.89
Crystal color, form	Gold, irregular block	Gold, needle	Gold/orange, irregular block	Gold, prism
Crystal system	Orthorhombi	Monoclinic	Monoclinic	Triclinic
Space group	*Pbca*	*C*2/*c*	*P*2(1)/*c*	$P\bar{1}$
a (Å)	15.1425(12)	23.272(2)	14.630(5)	9.6552(14)
b (Å)	14.8406(12)	17.8223(18)	13.661(4)	12.6354(18)
c (Å)	28.037(2)	15.6177(16)	9.700(3)	16.679(2)
α (°)	90	90	90	92.801(3)
β (°)	90	105.655(2)	108.921(7)	95.282(3)
γ (°)	90	90	90	106.263(3)
V ($Å^3$)	6300.6(8)	6237.3(10)	1833.9(10)	1939.1(5)
Z	8	4	4	2
Density (g/cm^3)	1.897	1.839	1.979	1.685
Absorption $\mu(mm^{-1})$	4.344	4.524	7.583	3.537
F(000)	3488	3376	1048	968
Crystal size (mm)	$0.35 \times 0.34 \times 0.30$	$0.18 \times 0.03 \times 0.03$	$0.26 \times 0.26 \times 0.14$	$0.28 \times 0.20 \times 0.05$
Temperature (°C)	−100	−100	−100	−100
Scan mode	ω	ω	ω	ω
Detector	Bruker-CCD	Bruker-CCD	Bruker-CCD	Bruker-CCD
θ_{max} (°)	28.48	28.3	28.35	28.3
Number of observed reflections	92832	57973	29810	35385
Number of unique reflections	7951	7706	4487	9331
R_{merge}	0.067	0.044	0.030	0.048
Number of parameters	475	389	221	513
S[a]	1.018	1.037	0.984	1.031
R indices $[I > 2\sigma(I)]$[b]	$wR_2 = 0.047$, $R_1 = 0.026$	$wR_2 = 0.063$, $R_1 = 0.027$	$wR_2 = 0.053$, $R_1 = 0.021$	$wR_2 = 0.076$, $R_1 = 0.034$
R indices (all data)[b]	$wR_2 = 0.054$, $R_1 = 0.046$	$wR_2 = 0.069$, $R_1 = 0.050$	$wR_2 = 0.056$, $R_1 = 0.026$	$wR_2 = 0.080$, $R_1 = 0.045$
Maximum difference in peak and hole ($e/Å^3$)	0.912, −0.555	1.792, −0.715	1.975, −0.963	2.682, −1.072

[a] $GooF = S = \{\sum[w\,(F_o^2 - F_c^2)^2]/(n\text{-}p)\}^{1/2}$, where *n* is the number of reflections, and *p* is the total number of refined parameters.
[b] $R_1 = \sum||F_o| - |F_c||/\sum|F_o|$, $wR_2 = \{\sum[w(F_o^2 - F_c^2)^2]/\sum[w(F_o^2)^2]\}^{1/2}$ (sometimes denoted as R_w2).

Table 3
Summary of crystal data, data collection, and structural refinement parameters for **15**, **17** and **19**

	15	**17**	**19**
Empirical formula	$C_{38}H_{34}F_{12}IrN_2O_2P$	$C_{38}H_{26}F_{19}IrN_2O_2$	$C_{36}H_{20}F_{18}IrN_3O$
FW	1001.84	1095.81	1044.75
Crystal color, form	Gold, needle	Gold, prism	Gold, flat needle
Crystal system	Monoclinic	Orthorhombic	Monoclinic
Space group	*C*2/*c*	*Pbca*	*P*2(1)/*c*
a (Å)	15.719(7)	20.5488(14)	10.2856(16)
b (Å)	13.295(6)	15.8771(11)	22.089(3)
c (Å)	18.608(9)	23.7910(16)	15.929(3)
α (°)	90	90	90
β (°)	90.862(8)	90	90.221(2)
γ (°)	90	90	90
V (Å^3)	3888(3)	7761.9(9)	3619.0(10)
Z	4	8	4
Density (g/cm^3)	1.711	1.875	1.917
Absorption M (mm^{-1})	3.569	3.57	3.818
F(000)	1968	4256	2016
Crystal size (mm)	$0.26 \times 0.05 \times 0.03$	$0.32 \times 0.09 \times 0.08$	$0.48 \times 0.13 \times 0.02$
Temperature (°C)	−100	−100	−100
Scan mode	*ω*	*ω*	*ω*
Detector	Bruker-CCD	Bruker-CCD	Bruker-CCD
θ_{max} (°)	28.36	28.63	27.4
Number of observed reflections	22 701	151 983	61 857
Number of unique reflections	4701	9933	8207
R_{merge}	0.0424	0.1018	0.0928
Number of parameters	258	564	545
S[a]	1.061	1.005	1.03
R indices [$I > 2\sigma(I)$][b]	$wR_2 = 0.071$, $R_1 = 0.032$	$wR_2 = 0.059$, $R_1 = 0.032$	$wR_2 = 0.070$, $R_1 = 0.036$
R indices (all data)[b]	$wR_2 = 0.077$, $R_1 = 0.043$	$wR_2 = 0.069$, $R_1 = 0.062$	$wR_2 = 0.079$, $R_1 = 0.062$
Maximum difference in peak and hole (e/Å^3)	1.884, −0.792	1.363, −1.091	2.488, −0.909

[a] GooF $= S = \{\sum[w\,(F_o^2 - F_c^2)^2]/(n\text{-}p)\}^{1/2}$, where *n* is the number of reflections, and *p* is the total number of refined parameters.
[b] $R_1 = \sum\|F_o| - |F_c\|/\sum|F_o|$, $wR_2 = \{\sum[w(F_o^2 - F_c^2)^2]/\sum[w(F_o^2)^2]\}^{1/2}$ (sometimes denoted as R_w2).

There is also an apparent correlation between the radiance and the theta angle. Compound **23** has the smallest theta angle and the lowest efficiency and radiance, while compound **21** has the largest theta angle and the highest efficiency and radiance.

5. Experimental

5.1. General procedures

All operations were carried out under an argon atmosphere using standard Schlenk techniques unless otherwise indicated. Organic solvents were distilled from drying agents or passed through alumina columns under an argon or nitrogen atmosphere. 3,5-Bis(trifluoromethyl)phenylboronic acid, 2-chloro-4-methylpyridine, Pd_2dba_3, cesium fluoride, 1,4-dioxane, lithium 2,4-pentanedionate, lithium 2,2,6,6-tetramethyl-heptane-3,5-dionate, trimethylphosphate, rubidium hydroxide in water, benzoylformic acid, di-*tert*-butylchlorophosphine, (trimethylsilylmethyl)lithium, tris(trimethylsilyl)phosphine, pivaloyl chloride, and 2,2-dimethyl-6,6,7,7,8,8,8-heptafluoro-3,5-octadione were purchased from Aldrich. Iridium (III) chloride trihydrate was purchased from Alfa Aesar. 2,2-Bis(trifluoromethyl)-oxirane is a DuPont product. 2-[(Diphenylphosphanyl)-methyl]-1,1,1,3,3,3-hexafluoro-propan-2-ol was synthesized by the known addition of diphenylphosphine to 2,2-bis(trifluoromethyl)oxirane [36]. 2-Diphenylphosphanylethanol and 1-diphenylphosphanylpropan-2-ol were synthesized by the reaction of diphenylphosphine with the appropriate epoxy compounds [37]. Diphenylphosphanylmethanol was prepared by reaction of diphenylphosphine and formaldehyde [12]. Caution should be taken during the preparation of complex **30** due to the release of formaldehyde.

5.2. Di-tert-butyltrimethylsilanylmethylphosphine (*5*)

50.00 g (0.277 mol) of Di-*tert*-butylchlorophosphine, 304 ml of 1.0 M pentane solution of (trimethylsilylmethyl)lithium and 150 ml of THF were refluxed under argon for 3 days. The reaction mixture was allowed to cool to RT, and an aqueous solution of ammonium chloride was added slowly. The organic phase was separated, and then dried over magnesium sulfate. After removal of the solvent, the product was purified by distillation in vacuo. The yield of di-*tert*-butyltrimethylsilanylmethylphosphine was 55.32 g (86%) with b.p. 50–52 °C/0.5 mm. ^{1}H NMR (C_6D_6) 0.01 (s, 9H, $SiMe_3$), 0.23 (d, $^2J_{PH} = 5.34$ Hz, 2H,

Table 4
Summary of crystal data, data collection, and structural refinement parameters for **21**, **23** and **25**

	21	**23**	**25**
Empirical formula	$C_{36}H_{23}Cl_2F_{18}IrN_4O$	$C_{44}H_{38}F_{12}IrN_2O_3P$	$C_{48}H_{44}F_{12}IrN_2OP$
FW	1132.68	1093.93	1116.02
Crystal color, form	Yellow, irregular block	Gold, prism	Yellow, prism
Crystal system	Monoclinic	Triclinic	Monoclinic
Space group	$P2(1)/n$	$P\bar{1}$	$P2(1)/n$
a (Å)	12.2355(14)	11.2224(8)	11.7299(10)
b (Å)	24.179(3)	12.0442(8)	24.012(2)
c (Å)	12.8560(14)	17.2048(12)	17.0363(15)
α (°)	90	80.5150(15)	90
β (°)	96.586(2)	89.7810(15)	106.599(2)
γ (°)	90	66.0150(14)	90
V (Å^3)	3778.3(7)	2090.5(3)	4598.5(7)
Z	4	2	4
Density (g/cm^3)	1.991	1.738	1.612
Absorption μ (mm^{-1})	3.803	3.329	3.025
$F(000)$	2192	1080	2216
Crystal size (mm)	$0.17 \times 0.06 \times 0.04$	$0.34 \times 0.24 \times 0.20$	$0.23 \times 0.20 \times 0.20$
Tempearture (°C)	−100	−100	−100
Scan mode	ω	ω	ω
Detector	Bruker-CCD	Bruker-CCD	Bruker-CCD
θ_{max} (°)	28.28	28.3	28.28
Number of observed reflections	14106	39322	30257
Number of unique reflections	8037	10082	10905
R_{merge}	0.0254	0.0224	0.0336
Number of parameters	561	590	558
S[a]	1.034	1.021	1.064
R indices $[I > 2\sigma(I)]$[b]	$wR_2 = 0.066$, $wR_1 = 0.031$	$wR_2 = 0.043$, $R_1 = 0.017$	$wR_2 = 0.070$, $R_1 = 0.029$
R indices (all data)[b]	$wR_2 = 0.075$, $R_1 = 0.050$	$wR_2 = 0.044$, $R_1 = 0.019$	$wR_2 = 0.073$, $R_1 = 0.039$
Maximum difference in peak and hole (e/Å^3)	1.676, −0.928	1.174, −0.664	1.763, −1.437

[a] GooF $= S = \{\sum[w\,(F_o^2 - F_c^2)^2]/(n\text{-}p)\}^{1/2}$, where n is the number of reflections, and p is the total number of refined parameters.
[b] $R_1 = \sum\|F_o| - |F_c\|/\sum|F_o|$, $wR_2 = \{\sum[w(F_o^2 - F_c^2)^2]/\sum[w(F_o^2)^2]\}^{1/2}$ (sometimes denoted as R_w2).

P-CH_2-$SiMe_3$), 0.91 (s, 9H, Me_3C), 0.93 (s, 9H, Me_3C). ^{31}P NMR (C_6D_6) 20.05 (s, 1P). Anal. Calc. for $C_{12}H_{29}PSi$: C, 62.01; H, 12.58; P, 13.33. Found: C, 61.89; H, 12.53; P, 13.25%.

5.3. 2-(3,5-Bis(trifluoromethyl)phenyl)-4-methylpyridine (*1*)

Protocol A: 10.0 g (38 mmol) of 3,5-bis(trifluoromethyl)phenylboronic acid (**3**), 5 g (38 mmol) of 2-chloro-4-methylpyridine (**2**), 15 g of potassium carbonate, 0.5 g of tetrakis(triphenylphosphine)palladium (0), and 100 ml of 1,2-dimethoxyethane and 150 ml of water were refluxed (80–90 °C) for 16 h. The reaction mixture was diluted by 300 ml of water, extracted by dichloromethane (50 ml × 3), and washed by water (200 ml × 2). The organic layer was dried over magnesium sulfate, the solvent was removed under vacuum, and the residue was distilled under vacuum. A fraction with b.p. 66–68 °C/0.01 mm Hg was isolated (8 g, 52.5%). Based on ^1H NMR data, the purity of compound **1** was 94%.

Protocol B: 15.0 g (58.15 mmol) of 3,5-bis(trifluoromethyl)phenylboronic acid (**3**), 7.42 g (58.16 mmol) of 2-chloro-4-methylpyridine (**2**), 17.43 g (114.8 mmol) of cesium fluoride **7**, 0.53 g (0.579 mmol) of tris(dibenzylideneacetone) dipalladium (0) **6**, 0.33 g (1.42 mmol) of di-*tert*-butyltrimethylsilylmethylphosphine (**5**) and 100 ml of 1,4-dioxane were stirred at room temperature for 12 h. The reaction mixture was filtered and the solvent was removed under vacuo. The resulting mixture was purified by chromatography on silica gel with an eluent composed of petroleum ether/ethyl ether at 10/0.5. Yield of 2-(3,5-bis(trifluoromethyl)phenyl)-4-methylpyridine (**1**) was 16.18 g (91%) as a colorless liquid. ^1H NMR ($CDCl_3$) 2.56 (s, 3H, Me), 7.11 (s, 1H, arom-H), 7.51 (s, 1H, arom-H), 7.90 (s, 1H, arom-H), 8.45-8.55 (m, 3H, arom-H). ^{19}F NMR ($CDCl_3$) −63.35 (s, 3F, CF_3), −63.36 (s, 3F, CF_3). Anal. Calc. for $C_{14}H_9F_6N$: C, 55.09; H, 2.97; N, 4.59. Found: C, 55.01; H, 3.12; N, 4.44%.

5.4. Iridium, di-μ-chlorotetrakis[4,6-bis(trifluoromethyl)-2-(4-methyl-2-pyridinyl-κN)phenyl-κC]di (*8*)

12.38 g (40.6 mmol) of 2-(3,5-bis(trifluoromethyl)-phenyl)-4-methylpyridine, 5.47 g (15.5 mmol) of iridium (III) chloride trihydrate, and 40 ml of trimethylphosphate were stirred at 90 °C for 6 h under a flow of nitrogen. The precipitate was filtered and dried in vacuo at 1 mmHg. The yield of chlorodimer was 16.96 g (84%) as a yellow powder. The crude chlorodimer was used "as is" in the next steps.

Table 5
Summary of crystal data, data collection, and structural refinement parameters for **28**, **29** and **33**

	28	**29**	**33**
Empirical formula	$C_{40}H_{27}ClF_{12}IrN_2P$	$C_{56}H_{48}ClF_{12}IrN_2O_2P_2$	$C_{30}H_{31}F_{12}IrN_2O_3S_2$
FW	1022.26	1298.55	951.89
crystal color, form	Yellow, irreg block	Gold, needle	Gold, irreg. Block
Crystal system	Triclinic	Triclinic	Triclinic
Space group	$P\bar{1}$	$P\bar{1}$	$P\bar{1}$
a (Å)	11.6057(17)	11.364(3)	14.388(7)
b (Å)	11.6433(17)	12.288(3)	14.766(7)
c (Å)	18.297(3)	19.859(5)	17.877(9)
α (°)	88.537(2)	102.765(5)	78.882(9)
β (°)	74.304(2)	103.042(5)	80.718(9)
γ (°)	81.146(3)	98.554(4)	76.906(10)
V (Å^3)	2351.6(6)	2576.8(12)	3602(3)
Z	2	2	4
Density (g/cm^3)	1.444	1.674	1.755
Absorption μ(mm^{-1})	3.004	2.794	3.918
F(000)	996	1292	1864
Crystal size (mm)	$0.22 \times 0.22 \times 0.14$	$0.15 \times 0.02 \times 0.01$	$0.14 \times 0.14 \times 0.12$
Temperature (°C)	−100	−100	−100
Scan mode	ω	ω	ω
Detector	Bruker-CCD	Bruker-CCD	Bruker-CCD
θ_{max} (°)	28.3	28.31	28.26
Number of observed reflections	30865	16796	22193
Number of unique reflections	11029	11564	15529
R_{merge}	0.0357	0.0275	0.0403
Number of parameters	496	689	876
S[a]	1.019	1.043	1.098
R indices[$I > 2\sigma$(9iI)][b]	$wR_2 = 0.113$, $R_1 = 0.044$	$wR_2 = 0.090$, $R_1 = 0.039$	$wR_2 = 0.216$, $R_1 = 0.078$
R indices (all data)[b]	$wR_2 = 0.119$, $R_1 = 0.060$	$wR_2 = 0.099$, $R_1 = 0.058$	$wR_2 = 0.227$, $R_1 = 0.094$
Maximum difference in peak and hole (e/Å^3)	2.940, −0.881	2.751, −0.919	7.074, −3.185

[a] GooF $= S = \{\sum[w\,(F_o^2 - F_c^2)^2]/(n\text{-}p)\}^{1/2}$, where n is the number of reflections, and p is the total number of refined parameters.
[b] $R_1 = \sum\|F_o| - |F_c\|/\sum|F_o|$, $wR_2 = \{\sum[w(F_o^2 - F_c^2)^2]/\sum[w(F_o^2)^2]\}^{1/2}$ (sometimes denoted as R_w2).

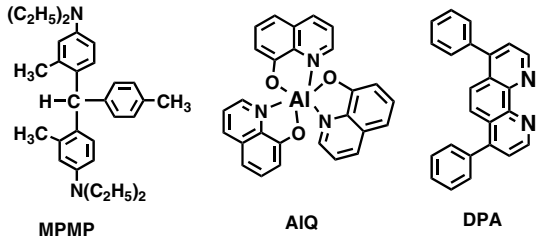

Scheme 14.

5.5. Iridium, bis[4,6-bis(trifluoromethyl)-2-(4-methyl-2-pyridinyl-κN)phenyl-κC](2,4-pentanedio-nato-κO,κO′) (9)

2.5 g (1.50 mmol) of Iridium, di-μ-chlorotetrakis[4,6-bis(trifluoromethyl)-2-(4-methyl-2-pyridinyl-κN)phenyl-κC]di- (**9**) 7.32 g (68.7 mmol) lithium 2,4-pentanedionate, and 30 ml of THF were refluxed for 2 h under an argon atmosphere. The reaction mixture was poured into 200 ml of water and extracted twice with 200 ml of diethyl ether. The extracts were dried over magnesium sulfate overnight. The solvent was removed on a rotoevaporator and the residue was purified by chromatography on silica gel with an eluent composed of petroleum ether/ethyl ether at 10/0.5. Three Ir complexes were isolated and characterized. Yield of iridium, bis[4,6-bis(trifluoromethyl)-2-(4-methyl-2-pyridinyl-κN)phenyl-κC](2,4-pentanedionato-κ*O*, κ*O*′)-, was 2.17 g (81%) as a yellow solid with m.p. 351.48 °C. ^{1}H NMR (CD_2Cl_2) 1.60 (s, 6H, Me), 2.55 (s, 3H, Me), 5.30 (s, 1H, H–C=), 6.90–8.10 (m, 10H, arom-H). ^{19}F NMR (CD_2Cl_2) −60.23 (s, 6F, CF_3), −63.00 (s, 6F, CF_3), Anal. Calc. for $C_{33}H_{23}F_{12}IrN_2O_2$ (Exact Mass:

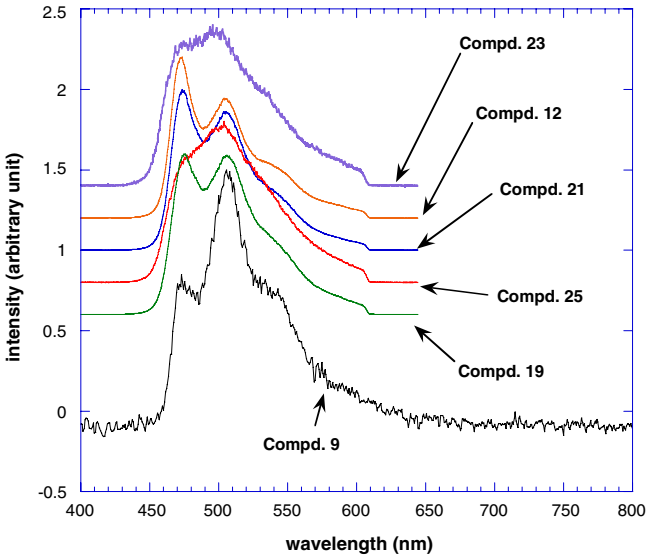

Fig. 11. Electroluminescent spectra of various Ir compounds.

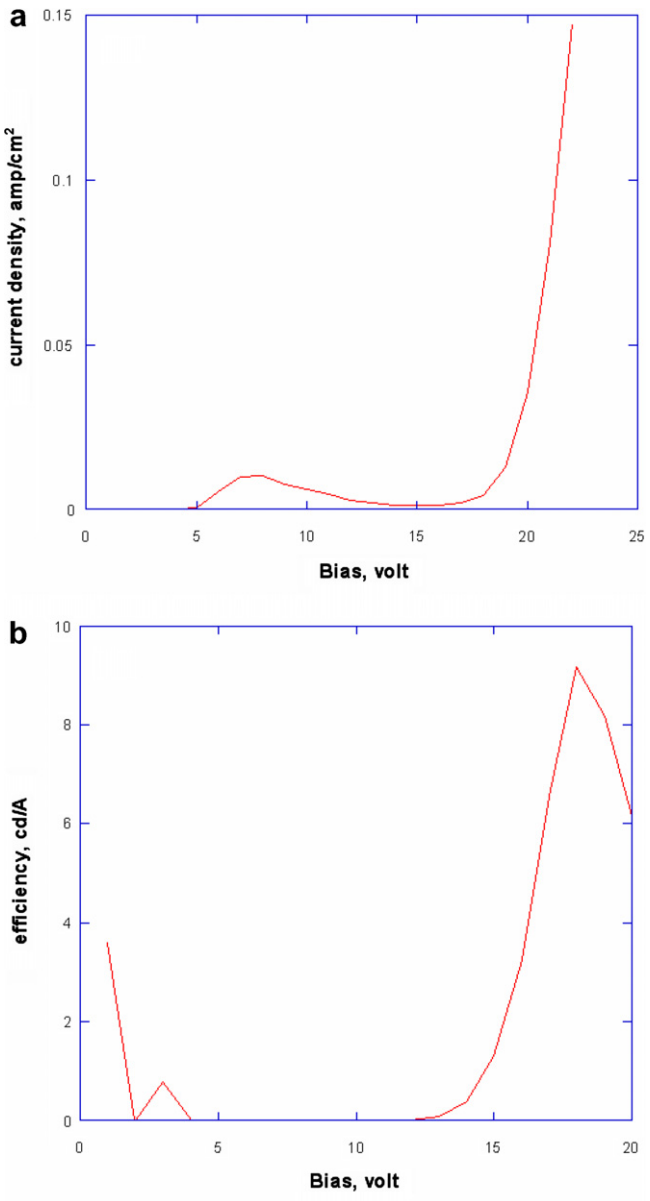

Fig. 12. (a) Current density vs. voltage curves; and (b) Efficiency vs. voltage of complex **21**.

900.12): C, 44.05; H, 2.58; N, 3.11. Found: C, 44.01; H, 2.51; N, 2.88%. Yield of iridium, [4,6-bis(trifluoromethyl)-2-(4-methyl-2-pyridinyl-κN)phenyl-κC],[2-(4-methyl-2-pyridinyl-κN)-6-methyl-3-pyridinyl-κC],(2,4-pentanedionato-κ*O*,κ*O*′)- (**10**) was 0.34 g (10%) as a yellow solid with no m.p. below 200 °C. ^{1}H NMR (CD_2Cl_2) 1.55 (br, 6H, Me), 2.45 (br, 3H, Me), 5.20 (s, 1H, H–C═), 6.90–8.10 (m, 9H, arom-H). ^{19}F NMR (CD_2Cl_2) −60.54 (s, 6F, CF_3), −63.07 (s, 6F, CF_3), Anal. Calc. for $C_{31}H_{26}F_6IrN_3O_2$ (Exact Mass: 779.16): C, 47.81; H, 3.37; N, 5.40. Found: C, 47.83; H, 3.07; N, 5.36%. Yield of iridium, dichloro,[4,4′-dimethyl-[2,2′]bipyridinyl-κN1,κN1], (2,4-pentanedionato-κ*O*,κ*O*′)-, (**11**) was 0.08 g (5%) as a few orange crystals with no m.p. below 200 °C. ^{1}H NMR (CD_2Cl_2) 1.55 (br, 6H, Me), 2.45 (br, 6H, Me), 5.21 (s, 1H, H–Cdbond), 6.85–8.12 (m, 6H, arom-H). Anal. Calc. for $C_{17}H_{19}Cl_2IrN_2O_2$ (Exact Mass: 546.05): C, 37.36; H, 3.50; N, 5.13. Found: C, 37.40; H, 3.73; N, 5.42%.

*5.6. Iridium,bis[4,6-bis(trifluoromethyl)-2-(4-methyl-2-pyridinyl-κN)phenyl-κC](2,2,6,6-tetramethyl-3,5-heptanedionato-κO,κO′) (**12**)*

2.5 g (1.50 mmol) of Iridium, di-μ-chlorotetrakis[4,6-bis(trifluoromethyl)-2-(4-methyl-2-pyridinyl-κN)phenyl-κC]di-, 5.91 g (31.1 mmol) lithium 2,2,6,6-tetramethyl-heptane-3,5-dionate, and 30 ml of THF were refluxed for 2 h under an argon atmosphere. The reaction mixture was poured into 200 ml of water and extracted twice with 200 ml of diethyl ether. The extracts were dried over magnesium sulfate overnight. The solvent was removed on a rotoevaporator and the residue was purified by chromatography on silica gel with an eluent composed of petroleum ether/ethyl ether at 10/0.5. Yield of iridium, bis[4,6-bis(trifluoromethyl)-2-(4-methyl-2-pyridinyl-κN)phenyl-κC](2,2,6,6-tetramethyl-3,5-heptanedionato-κ*O*,κ*O*′)-, was 1.97 g (67%) as a yellow solid with m.p. 306.53 °C. ^{1}H NMR (CD_2Cl_2) 0.80 (s, 18H *t*-Bu), 2.50 (s, 6H, Me), 5.40 (s, 1H, H–C═), 6.40–8.10 (m, 10H, arom-H).^{19}F NMR (CD_2Cl_2) −60.26 (s, 6F, CF_3), −62.83 (s, 6F, CF_3), Anal. Calc. $C_{39}H_{35}F_{12}IrN_2O_2$ (Mol. Wt.: 983.91): C, 47.61; H, 3.59; N, 2.85. Found: C, 47.55; H, 3.60; N, 2.78%. The structure was determined by X-ray analysis.

*5.7. Iridium,bis[4,6-bis(trifluoromethyl)-2-(4-methyl-2-pyridinyl-κN)phenyl-κC],((2,2-dimethyl-1-oxopropyl)phosphinato-O,O′) (**15**)*

1.0 g (0.6 mmol) of Iridium, di-μ-chlorotetrakis[4,6-bis-(trifluoromethyl)-2-(4-methyl-2-pyridinyl-κN)phenyl-κC]di-, 0.95 g (3.45 mmol) of dipivaloyltrimethylsilylphosphine, and 30 ml of THF were refluxed for 2 h under an argon atmosphere. The solvent was removed on a rotoevaporator and the residue was purified by chromatography on silica gel with an eluent composed of petroleum ether/ethyl ether at 10/0.5. Yield of iridium,bis[4,6-bis(trifluoromethyl)-2-(4-methyl-2-pyridinyl-κN)phenyl-κC],((2,2-dimethyl-1-oxopropyl)phosphinato-*O*,*O*′)-, was 0.35 g (30%) as a yellow solid with no m.p. below 200 °C. ^{1}H NMR (CD_2Cl_2) 0.75 (s, 18H, Me), 1.65 (s, 6H, Me), 6.00–8.10 (m, 10H, arom-H). ^{19}F NMR (CD_2Cl_2) −59.51 (s, 6F, CF_3), −62.11 (s, 6F, CF_3). ^{31}P NMR (CD_2Cl_2) 50.97. ^{13}C NMR (CD_2Cl_2) (selected signals) + 240.23 (d, $^{1}J_{CP} = 108.8$ Hz, C═P). Anal. Calc. for $C_{38}H_{34}F_{12}IrN_2O_2P$ (Mol. Wt.: 1001.86): C, 45.56; H, 3.42; N, 2.80. Found: C, 45.50; H, 3.79; N, 3.09%. The structure was determined by X-ray analysis.

*5.8. Iridium,bis[4,6-bis(trifluoromethyl)-2-(4-methyl-2-pyridinyl-κN)phenyl-κC], (6,6,7,7,8,8,8-heptafluoro-2,2-dimethyl-3,5-octanedionato-κO,κO′) (**17**)*

1.0 g (0.6 mmol) of Iridium, di-μ-chlorotetrakis[4,6-bis-(trifluoromethyl)-2-(4-methyl-2-pyridinyl-κN)phenyl-κC]di-,

0.51 g (1.72 mmol) of 2,2-dimethyl-6,6,7,7,8,8,8-heptafluoro-3,5-octadione, 0.64 g (6.2 mmol) of rubidium hydroxide in 5 ml of water, and 40 ml of 1,2-dichloroethane were refluxed for 2 h under an argon atmosphere. The reaction mixture was poured into 200 ml of water and extracted twice with 200 ml of diethyl ether. The extracts were dried over magnesium sulfate overnight. The solvent was removed on a rotoevaporator and the residue was purified by chromatography on silica gel with an eluent composed of petroleum ether/ethyl ether at 10/0.5. Yield of iridium, bis[4,6-bis(trifluoromethyl)-2-(4-methyl-2-pyridinyl-κN)-phenyl-κC],(6,6,7,7,8,8,8-heptafluoro-2,2-dimethyl-3,5-octanedionato-κ*O*,κ*O*′)-, was 0.37 g (30%) as a yellow solid with no m.p. below 200 °C. ^{1}H NMR (CD_2Cl_2) 0.80 (s, 9H, Me), 2.60 (s, 6H, Me), 5.70 (s, 1H, H–C═), 6.50–8.10 (m, 10H, arom-H). ^{19}F NMR (CD_2Cl_2) −60.08 (s, 6F, CF_3), −63.03 (s, 6F, CF3), −81.15 (s, 3F, CF_3), −119.02 (m, 2F, CF_2), −127.07 (m, 2F, CF_2). Anal. Calc. $C_{38}H_{26}F_{19}IrN_2O_2$ (Mol. Wt.: 1095.81): C, 41.65; H, 2.39; F, N, 2.56. Found: C, 41.66; H, 2.39; N, 2.72%.

5.9. Iridium,bis[4,6-bis(trifluoromethyl)-2-(4-methyl-2-pyridinyl-κN)phenyl-κC],[α,α-bis(trifluoromethyl)-2-pyridinemethanolato-κN1,κO2] (**19**)

0.9 g (0.54 mmol) of Iridium, di-μ-chlorotetrakis[4,6-bis(trifluoromethyl)-2-(4-methyl-2-pyridinyl-κN)phenyl-κC]di-, 0.50 g (2.03 mmol) of 1,1,1,3,3,3-hexafluoro-2-pyridin-2-yl-propan-2-ol, 0.60 g (5.9 mmol) of rubidium hydroxide in 5 ml of water, and 40 ml of 1,2-dichloroethane were refluxed for 2 h under an argon atmosphere. The reaction mixture was poured into 200 ml of water and extracted twice with 200 ml of diethyl ether. The extracts were dried over magnesium sulfate overnight. The solvent was removed on a rotoevaporator and the residue was purified by chromatography on silica gel with an eluent composed of petroleum ether/ethyl ether at 10/0.5. Yield of iridium, bis[4,6-bis(trifluoromethyl)-2-(4-methyl-2-pyridinyl-κN)-phenyl-κC],[α,α-bis(trifluoromethyl)-2-pyridinemethanolato-κN1,κO2], was 0.73 g (65%) as a yellow solid with no m.p. below 200 °C. ^{1}H NMR (CD_2Cl_2) 2.40 (s, 6H, Me), 6.50–8.70 (m, 14H, arom-H). ^{19}F NMR (CD_2Cl_2) −59.32 (s, 3F, CF_3), −59.63 (s, 3F, CF_3), −62.98 (s, 3F, CF_3), −63.01 (s, 3F, CF_3), −72.43 (s, 3F, CF_3), −76.59 (s, 3F, CF_3). Anal. Calc. for $C_{36}H_{20}F_{18}IrN_3O$ (Mol. Wt.: 1044.75): C, 41.39; H, 1.93; N, 4.02. Found: C, 41.49; H, 2.11; N, 4.73%.

5.10. Preparation of 1,1,1,3,3,3-hexafluoro-2-pyrazol-1-ylmethyl-propan-2-ol (**20**)

To a mixture of 13 g of KOH (pellets), 100 mL of THF, and 0.2 g of $(C_4H_9)_4N^+HSO_4^-$,pyrazole (13.6 g, 0.2 mol) was added in one portion. The reaction mixture was agitated at ambient temperature for 1 h and cooled to 5 °C. 38 g (0.21 mol) of 2,2-bis(trifluoromethyl)oxirane was slowly added (∼1 h) at 5–15 °C. The clear solution was agitated for another hour at 15 °C, and then ∼100 mL 10% hydrochloric acid was added to the reaction mixture over a 30 min period to bring pH to 3.5. The reaction mixture was diluted with 300 ml of water, and extracted with dichloromethane (100 ml × 2). The extract was dried over magnesium sulfate, and the solvent was removed under reduced pressure to give 47 g (95%) of white crystalline 1,1,1,3,3,3-hexafluoro-2-pyrazol-1-ylmethyl-propan-2-ol, m.p. 80 °C (from hexane, DSC), purity >99%.

^{1}H NMR ($CDCl_3$): 4.62 (s, 2H), 6.31(t, 1H, 2 Hz), 7.24 (s, br, 1H), 7.47 (d, 1H, 2 Hz), 7.64 (d, 1 H, 2 Hz). ^{19}F NMR ($CDCl_3$): −77.11(s). ^{13}C NMR ($CDCl_3$): 49.08 (hept, 2.2 Hz), 76.83 (hept., 29 Hz), 107 (s), 14.56 (q, 289 Hz), 132.10, 141.78. MS (*m*/*z*) 248 (M^+, $C_7H_6F_6N_2O^+$). Anal. Calc. for $C_7H_6F_6N_2O$: C, 33.88, H2.44, N, 11.11. Found: C, 33.90, H2.42, N, 11.29%.

5.11. Iridium,bis[4,6-bis(trifluoromethyl)-2-(4-methyl-2-pyridinyl-κN)phenyl-κC],[α,α-bis(trifluoromethyl)-2-pyrazol-1-ylmethyl- propan-2-olato-κN1,κO2] (**21**)

1.0 g (0.6 mmol) of Iridium, di-μ-chlorotetrakis[4,6-bis-(trifluoromethyl)-2-(4-methyl-2-pyridinyl-κN)phenyl-κC]di-, 0.43 g (1.73 mmol) of 1,1,1,3,3,3-hexafluoro-2-pyrazol-1-ylmethyl-propan-2-ol, 0.60 g (5.9 mmol) of rubidium hydroxide in 5 ml of water, and 40 ml of 1,2-dichloroethane were refluxed for 2 h under an argon atmosphere. The reaction mixture was poured into 200 ml of water and extracted twice with 200 ml of diethyl ether. The extracts were dried over magnesium sulfate overnight. The solvent was removed on a rotoevaporator and the residue was purified by chromatography on silica gel with an eluent composed of petroleum ether/ethyl ether at 10/0.5. Yield of iridium, bis[4,6-bis(trifluoromethyl)-2-(4-methyl-2-pyridinyl-κN)-phenyl-κC],[α,α-bis(trifluoromethyl)-2-pyrazol-1-ylmethyl-propan-2-olato-κN1,κO2], was 0.74 g (59%) as a yellow solid with no m.p. below 200 °C. ^{1}H NMR (CD_2Cl_2) 2.50 (s, 6H, Me), 3.80 (s, 1H, CH_2), 4.30 (s, 1H, CH_2), 6.10–8.60 (m, 13H, arom-H). ^{19}F NMR (CD_2Cl_2) −59.13 (s, 3F, CF_3), −59.35 (s, 3F, CF_3), −62.96 (s, 3F, CF_3), −63.03 (s, 3F, CF_3), −75.17 (s, 3F, CF_3), −78.60 (s, 3F, CF_3). Anal. Calc. for $C_{35}H_{21}F_{18}IrN_4O$ (Mol. Wt.: 1047.76): C, 40.12; H, 2.02; N, 5.35. Found: C, 39.89; H, 2.27; N, 5.01%. The structure was determined by X-ray analysis.

5.12. Iridium,bis[4,6-bis(trifluoromethyl)-2-(4-methyl-2-pyridinyl-κN)phenyl-κC],[3-(di-phenylphosphino)-1-propanolato-O,P] (**23**)

1.0 g (0.6 mmol) of Iridium, di-μ-chlorotetrakis[4,6-bis(trifluoromethyl)-2-(4-methyl-2-pyridinyl-κN)phenyl-κC] di-, 0.34 g (1.48 mmol) of 2-diphenylphosphanylethanol, 0.60 g (5.9 mmol) of rubidium hydroxide in 5 ml of water, and 40 ml of 1,2-dichloroethane were refluxed for 2 h under an argon atmosphere. The reaction mixture was poured into 200 ml of water and extracted twice with 200 ml of diethyl ether. The extracts were dried over magnesium sul-

fate overnight. The solvent was removed on a rotoevaporator and the residue was purified by chromatography on silica gel with an eluent composed of petroleum ether/ethyl ether at 10/0.5. Yield of iridium, bis[4,6-bis(trifluoromethyl)-2-(4-methyl-2-pyridinyl-κN)phenyl-κC],[3-(di-phenylphosphino)-1-propanolato-O,P], was 0.44 g (34%) as a yellow solid with no m.p. below 200 °C. ^{1}H NMR (CD_2Cl_2) 2.30 (s, 6H, Me), 2.35 (br, 1H, CH_2–P), 2.35 (br, 1H, CH_2–P), 3.80–4.10, (m, 2H, CH2–O), 6.10–8.60 (m, 15H, arom-H). ^{19}F NMR (CD_2Cl_2) −58.76 (s, 3F, CF_3), −60.89 (s, 3F, CF_3), −62.57 (s, 3F, CF_3), −63.06 (s, 3F, CF_3). ^{31}P NMR (CD_2Cl_2) 11.93 (s, 1P). Anal. Calc. for $C_{42}H_{30}F_{12}IrN_2OP$ (Mol. Wt.: 1029.87): C, 48.98; H, 2.94; N, 2.72. Found: C, 49.10; H, 2.47; N, 3.01%. The structure was determined by X-ray analysis.

5.13. Iridium,bis[4,6-bis(trifluoromethyl)-2-(4-methyl-2-pyridinyl-κN)phenyl-κC],[1-(di-phenylphosphino)-2-propanolato-O,P] (25)

1.0 g (0.6 mmol) of Iridium, di-μ-chlorotetrakis[4,6-bis-(trifluoromethyl)-2-(4-methyl-2-pyridinyl-κN)phenyl-κC]di- 0.37 g (1.51 mmol) of 1-diphenylphosphanylpropan-2-ol, 0.60 g (5.9 mmol) of rubidium hydroxide in 5 ml of water, and 40 ml of 1,2-dichloroethane were refluxed for 2 h under an argon atmosphere. The reaction mixture was poured into 200 ml of water and extracted twice with 200 ml of diethyl ether. The extracts were dried over magnesium sulfate overnight. The solvent was removed on a rotoevaporator and the residue was purified by chromatography on silica gel with an eluent composed of petroleum ether/ethyl ether at 10/0.5. Yield of iridium, bis[4,6-bis(trifluoromethyl)-2-(4-methyl-2-pyridinyl-κN)phenyl-κC],[1-(di-phenylphosphino)-2-propanolato-O,P], was 0.87 g (70%) as a yellow solid with no m.p. below 200 °C. ^{1}H NMR (CD_2Cl_2) 1.20 (s, 3H, Me), 2.30 (s, 6H, Me), 2.35 (br, 1H, CH_2–P), 2.35 (br, 1H, CH_2–P), 2.80 (m, 1H, CH_2–O), 6.10–8.60 (m, 15H, arom-H). ^{19}F NMR (CD_2Cl_2) −59.93 (s, 3F, CF_3), −60.86 (s, 3F, CF_3), −62.63 (s, 3F, CF_3), −63.07 (s, 3F, CF_3). ^{31}P NMR (CD_2Cl_2) 9.33 (s, 1P). Anal. Calc. for $C_{43}H_{32}F_{12}IrN_2OP$ (Mol. Wt.: 1043.90): C, 49.47; H, 3.09; N, 2.68. Found: C, 49.53; H, 3.25; N, 2.88%. The structure was determined by X-ray analysis.

5.14. Iridium,chlorobis[4,6-bis(trifluoromethyl)-2-(4-methyl-2-pyridinyl-κN)phenyl-κC],[diphenylphosphine] (28)

1.0 g (0.6 mmol) of Iridium, di-μchlorotetrakis[4,6-bis(trifluoromethyl)-2-(4-methyl-2-pyridinyl-κN)phenyl-κC]di-, 0.32 g (4.8 mmol) of diphenylphosphanylmethanol, 0.60 g (5.9 mmol) of rubidium hydroxide in 5 ml of water, and 30 ml of 1,2-dichloroethane were refluxed for 2 h under an argon atmosphere. The reaction mixture was poured into 200 ml of water and extracted twice with 200 ml of diethyl ether. The extracts were dried over magnesium sulfate overnight. The solvent was removed on a rotoevaporator and the residue was purified by chromatography on silica gel with an eluent composed of petroleum ether/ethyl ether at 10/0.5. Yield of iridium, chlorobis[4,6-bis(trifluoromethyl)-2-(4-methyl-2-pyridinyl-κN)phenyl-κC],[diphenylphosphine] (**28**) was 0.33 g (27%) as a yellow solid with no m.p. below 200 °C. ^{1}H NMR (CD_2Cl_2) 2.40 (br, 6H, Me), 6.10–8.50 (m, 15H, arom-H). ^{19}F NMR (CD_2Cl_2) −60.80 (br, 6F, CF_3), −63.09 (br, 6F, CF_3). ^{31}P NMR (CD_2Cl_2) −12.11 (s, 1P). Anal. Calc. for $C_{40}H_{27}ClF_{12}IrN_2P$ (Mol. Wt.: 1022.28): C, 47.00; H, 2.66; N, 2.74. Found: C, 47.28; H, 2.70; N, 2.89%. The structure was determined by X-ray analysis. Yield of iridium,bis[4,6-bis(trifluoromethyl)-2-(4-methyl-2-pyridinyl-κN)phenyl-κC],[1,2-ethanediylbis[diphenyl-phosphine]-κP,κP′], chloride (**29**) was 0.58 g (41%) as a yellow solid with no m.p. below 200 °C. ^{1}H NMR (CD_2Cl_2) 2.40 (br, 6H, Me), 3.10 (br, 4H, CH_2–P), 5.90–8.40 (m, 30H, arom-H). ^{19}F NMR (CD_2Cl_2) −61.37 (br, 6F, CF_3), −65.73 (br, 6F, CF_3). ^{31}P NMR (CD_2Cl_2) 23.44 (s, 1P). Anal. Calc. for $C_{54}H_{40}ClF_{12}IrN_2P_2$ (Mol. Wt.: 1234.51): C, 52.54; H, 3.27; N, 2.27. Found: C, 52.73; H, 3.49; N, 2.41%. The structure was determined by X-ray analysis.

5.15. Iridium,di-μ-hydroxytetrakis[4,6-bis(trifluoromethyl)-2-(4-methyl-2-pyridinyl-κN)phenyl-κC]di- (33)

1.0 g (0.6 mmol) of Iridium, di-μ-chlorotetrakis[4,6-bis(trifluoromethyl)-2-(4-methyl-2-pyridinyl-κN)phenyl-κC]di-, 0.35 g (2.3 mmol) of benzoylformic acid, 0.60 g (5.9 mmol) of rubidium hydroxide in 5 ml of water, and 40 ml of 1,2-dichloroethane were refluxed for 2 h under an argon atmosphere. The precipitate was filtered off, washed with 20 ml of water and recrystallized from DMSO. Yield of iridium, di-μ-hydroxytetrakis[4,6-bis-(trifluoromethyl)-2-(4-methyl-2-pyridinyl-κN)phenyl-κC]di-, was 0.67 g (69%) as a yellow solid with no m.p. below 200 °C. ^{1}H NMR (CD_2Cl_2) 2.60 (s, br., 6H, Me), 6.10–8.50 (m, 15H, arom-H). ^{19}F NMR (CD_2Cl_2) −58.97 (br, 6F, CF_3), −63.11 (br, 6F, CF_3). Anal. Calc. for $C_{56}H_{34}F_{24}Ir_2N_4O_2$ (Mol. Wt.: 1635.30): C, 41.13; H, 2.10; N, 3.43. Found: C, 41.20; H, 2.10; N, 3.49%. The structure was determined by X-ray analysis.

5.16. X-ray diffraction studies

Data for all structures were collected using a Bruker CCD system at −100 °C. Structure solution and refinement were performed using the SHELXTL [38] set of programs. The PLATON-SQUEEZE [39] program was used to correct the data where the solvent molecules could not be correctly modeled. The structural parameters are reported in Tables 1–4.

5.17. OLED device fabrication and characterization

OLED devices were fabricated by a thermal evaporation technique. The base vacuum for all thin film deposition was approximately 10^{-6} Torr. The deposition chamber was capable of depositing eight different films without the need to break

the vacuum. Patterned indium tin oxide (ITO) coated glass substrates from Thin Film Devices, Inc. were used. These ITOs are based on Corning 1737 glass coated with a 1400 Å ITO coating, and have a sheet resistance of 30 ohms/square and 80% light transmission. The patterned ITO substrates were cleaned ultrasonically in an aqueous detergent solution, rinsed with distilled water, then by 2-propanol, and finally degreased in toluene vapor for ~3 h before use.

The cleaned, patterned ITO substrate was then loaded into the vacuum chamber, and the chamber was pumped down to 10^{-6} Torr. The substrate was then further cleaned using an oxygen plasma for about 5 min. After cleaning, multiple layers of thin films were deposited sequentially onto the substrate by thermal evaporation. Patterned metal electrodes (Al or LiF/Al) or bipolar electrodes were deposited through a mask. The thickness of the film was measured during deposition using a quartz crystal monitor (Sycon STC-200). All film thickness reported in this study are nominal, calculated assuming the density of the material deposited to be one. The completed OLED device was taken out of the vacuum chamber and characterized immediately without encapsulation.

The OLED samples were characterized by measuring their: (1) current–voltage (*I–V*) curves, (2) electroluminescence radiance versus voltage, and (3) electroluminescence spectra versus voltage The *I–V* curves were measured with a Source-Measurement Unit (Keithley Model 237, USA). The electroluminescence radiance (in units of cd/m^2) vs. voltage was measured with a luminescence meter (Minolta LS-110, Japan), while the voltage was scanned using the Keithley SMU. The electroluminescence spectrum was obtained by collecting light using an optical fiber, through an electronic shutter, dispersed through a spectrograph, and then measured with a diode array detector. All three measurements were performed at the same time and controlled by a computer. The efficiency of the device at a certain voltage is determined by dividing the electroluminescence radiance of the LED by the current density needed to run the device. The unit is in cd/A.

6. Supplementary material

CCDC 637999, 638000, 638001, 638002, 638003, 638004, 638005, 638006, 638007, 638008, 638009, 638010 and 638011 contain the supplementary crystallographic data for **9**, **10**, **11**, **12**, **15**, **17**, **19**, **21**, **23**, **25**, **28**, **29** and **33**. These data can be obtained free of charge via http://www.ccdc.cam.ac.uk/conts/retrieving.html, or from the Cambridge Crystallographic Data Centre, 12 Union Road, Cambridge CB2 1EZ, UK; fax: (+44) 1223-336-033; or e-mail: deposit@ccdc.cam.ac.uk.

Acknowledgements

The authors thank Kurt Adams for funding X-ray research, and Karin Karel for valuable suggestions and proofreading the manuscript.

References

[1] S. Tennant, Phil. Trans. R. Soc. 94 (1804) 411.
[2] (a) M. Zhao, J.L. Bada, Nature 339 (1989) 463;
(b) S. Bajpai, G.V.R. Prasad, J. Geolog. Soc. 157 (2000) 257;
(c) B.F. Bohor, D.M. Triplehorn, D.J. Nichols, H.T. Millard, Geology 15 (1987) 896.
[3] (a) S. Lamansky, P. Djurovich, D. Murphy, F. Abdel-Razzaq, H.E. Lee, C. Adachi, P.E. Burrows, S.R. Forrest, M.E. Thompson, J. Am. Chem. Soc. 123 (2001) 4304;
(b) M.A. Baldo, D.F. O'Brien, Y. You, A. Shoustikov, S. Sibley, M.E. Thompson, S.R. Forrest, Nature 395 (1998) 151.
[4] A.S. Ionkin, W.J. Marshall, Y. Wang, Organometallics 24 (2005) 619.
[5] V. Grushin, V.A. Petrov, PCT Int. Appl. (2003) WO 2003069961.
[6] A. Suzuki, Chem. Commun. 38 (2005) 4759.
[7] (a) M. Lepeltier, T.K.-M. Lee, K.K.-W. Lo, L. Toupet, H. Le Bozec, V. Guerchais, Eur. J. Inorg. Chem. 1 (2005) 110;
(b) A.J.S. Bexon, J.A.G. Williams, Comp. Rendus Chimie 8 (2005) 1326.
[8] (a) A.S. Ionkin, W.J. Marshall, D.C. Roe, Y. Wang, Dalton Trans. 20 (2006) 2468;
(b) A.S. Ionkin, W.J. Marshall, B.M. Fish, Organometallics 25 (2006) 1461;
(c) A.S. Ionkin, Y. Wang, U.S. Pat. Appl. Publ. (2005), 11 pp. US 2005244645 A1 20051103;
(d) A.S. Ionkin, Y. Wang, U.S. Pat. Appl. Publ. (2005), 9 pp. US 2005238910 A1 20051027;
(e) A.S. Ionkin, W.J. Marshall, J. Organomet. Chem. 689 (2004) 1057;
(f) A.S. Ionkin, U.S. Pat. Appl. Publ. (2006), 10 pp. US 2006281923 A1 20061214.
[9] (a) A.H. Cowley, N.C. Norman, M. Pakulski, Inorg. Synth. 27 (1990) 235;
(b) A.S. Ionkin, W.J. Marshall, Y. Wang, Organometallics 24 (2005) 619;
(c) A.S. Ionkin, W.J. Marshall, Organometallics 23 (2004) 6031;
(d) A.S. Ionkin, W.J. Marshall, Inorg. Chem. 44 (2005) 6244.
[10] G.Z. Becker, Anorg. Allgem. Chem. 430 (1977) 66.
[11] (a) A.S. Ionkin, L.F. Chertanova, B.A. Arbuzov, Phosphorus, Sulfur, Silicon 55 (1991) 133;
(b) G. Becker, M. Roessler, G. Uhl, Z. Anorg. Allgem. Chem. 495 (1982) 73;
(c) G. Becker, M. Niemeyer, O. Mundt, W. Schwarz, M. Westerhausen, M.W. Ossberger, P. Mayer, H. Noeth, Z. Zhong, P.J. Dijkstra, J. Feijen, Z. Anorg. Allg. Chem. 630 (2004) 2605.
[12] H. Hellmann, J. Bader, H. Birkner, O. Schumacher, Ann. 659 (1962) 49.
[13] (a) E.N. Tsvetkov, N.A. Bondarenko, I.G. Malakhova, M.I. Kabachnik, Synthesis 3 (1986) 198;
(b) M.T. Honaker, R.N. Salvatore, Phosphorus, Sulfur Silicon 179 (2004) 277;
(c) M.T. Honaker, B.J. Sandefur, J.L. Hargett, A.L. McDaniel, R.N. Salvatore, Tetrahedron Lett. 44 (2003) 8373.
[14] (a) K. Banholzer, H. Schmid, Angew. Chem. 69 (1957) 483;
(b) V.S. Srinivasan, E.S. Gould, Inorg. Chem. 20 (1981) 208;
(c) L.-T. Chen, G.-J. Chen, X.-Y. Fu, Chin. J. Chem. 13 (1995) 487.
[15] B. Schmid, F.O. Garces, R.J. Watts, Inorg. Chem. 33 (1994) 9.
[16] Q. Zhao, C.-Y. Jiang, M. Shi, F.-Y. Li, T. Yi, Y. Cao, C.-H. Huang, Organometallics 25 (2006) 3631.
[17] (a) I.R. Laskar, S.-F. Hsu, T.-M. Chen, Polyhedron 25 (2006) 1167;
(b) S. Lamansky, P. Djurovich, D. Murphy, F. Abdel-Razzaq, R. Kwong, I. Tsyba, M. Bortz, B. Mui, R. Bau, M.E. Thompson, Inorg. Chem. 40 (2001) 1704.
[18] (a) S. Yamaguchi, Organomet. News 3 (2005) 104;
(b) M.G. Colombo, A. Hauser, H.U. Gudel, Top. Curr. Chem. 171 (1994) 143.

[19] M.A. Baldo, S. Lamansky, P.E. Burrows, M.E. Thompson, S.R. Forrest, Appl. Phys. Lett. 75 (1999) 4.
[20] R.J. Holmes, S.R. Forrest, Y.-J. Tung, R.C. Kwong, J.J. Brown, S. Garon, M.E. Thompson, Appl. Phys. Lett. 82 (2003) 2422.
[21] C. Adachi, M.A. Baldo, S.R. Forrest, S. Lamansky, M.E. Thompson, R.C. Kwong, Apply. Phys. Lett. 78 (2001) 1622.
[22] V.V. Grushin, N. Herron, D.D. LeCloux, W.J. Marshall, V.A. Petrov, Y. Wang, Chem. Commun. (2001) 1494.
[23] Y. Wang, N. Herron, V.V. Grushin, D. LeCloux, V. Petrov, Appl. Phys. Lett. 79 (2001) 449.
[24] V.V. Grushin, D.D. LeCloux, V.A. Petrov, Y. Wang, U.S. Patent 6,670,645.
[25] Y.-J. Su, H.-L. Huang, C.-L. Li, C.-H. Chien, Y.-T. Tao, P.-T. Chou, S. Datta, R.-S. Liu, Adv. Mater. 15 (2003) 884.
[26] S.-C. Lo, N.A.H. Male, J.P.J. Markham, S.W. Magennis, P.L. Burn, O.V. Salata, I.D.W. Samuel, Adv. Mater. 14 (2002) 975.
[27] H.Z. Xie, M.W. Liu, O.Y. Wang, X.H. Zhang, C.S. Lee, L.S. Hung, S.T. Lee, P.F. Teng, H.L. Kwong, H. Zheng, C.M. Che, Adv. Mater. 13 (2001) 1245.
[28] J.-P. Duan, P.-P. Sun, C.-H. Cheng, Adv. Mater. 15 (2003) 224.
[29] T. Watanabe, K. Nakamura, S. Kawami, Y. Fukuda, T. Tsuji, T. Wakimoto, S. Miyaguchi, in: Kafafi, Z.H. (Ed.), Organic Light-emitting Materials and Devices IV, Proc. of SPIE, vol. 4105. The International Society for Optical Engineering; 2001, p. 175.
[30] M. Ikai, S. Tokito, Y. Sakamoto, T. Suzuki, Y. Taga, Apply. Phys. Lett. 79 (2001) 156.
[31] V. Adamovich, J. Brooks, A. Tamayo, A.M. Alexander, P.I. Djurovich, B.W. D'Andrade, C. Adachi, S.R. Forrest, M.E. Thompson, New J. Chem. 26 (2002) 1171.
[32] B.W. D'Andrade, J. Brooks, V. Adamovich, M.E. Thompson, S.R. Forrest, Adv. Mater. 14 (2002) 1033.
[33] W. Lu, B.-X. Mi, M.C.W. Chan, Z. Hui, N. Zhu, S.-T. Lee, C.-M. Che, Chem. Commun. (2002) 206.
[34] W. Lu, B.-X. Mi, M.C.W. Chan, Z. Hui, C.-M. Che, N. Zhu, S.-T. Lee, J. Am. Chem. Soc. 126 (2004) 4958.
[35] M. Born, E. Wolf, Principles of Optics, 6th ed., Pergamon Press, Oxford, 1980.
[36] V.V. Grushin, W.J. Marshall, G.A. Halliday, F. Davidson, V.A. Petrov, J. Fluorine Chem. 117 (2002) 121.
[37] K. Issleib, R. Reischel, Chem. Ber. 98 (1965) 2086.
[38] SHELXTL Software Suite, Version 5.1, G. Sheldrick, Bruker AXS Corp, Madison, WI.
[39] A.L. Spek PLATON, A Multipurpose Crystallographic Tool, Utrecht University, Utrecht, The Netherlands, 2005.